TEAMER
Testing & Expertise for Marine Energy

Test Plan

Additional Degree of Freedom for WEC

Awardee: Dehlsen Associates, LLC

Awardee point of contact: Alan McCall

Facility: Oregon State University WESRF

Facility point of contact: Ted Brekken

Date: 14 October 2020

TEAMER
Testing & Expertise for Marine Energy

EXECUTIVE SUMMARY

Dehlsen Associates' Centipod wave energy converter's (WEC) main potential design limitation is the inherent theoretical capture limit of a single degree of freedom (DoF) heaving point absorber. This TEAMER project aimed to leverage the expertise of Oregon State University WESRF's personnel to implement a second DoF in the existing model predictive control (MPC) optimization formulation, allowing Dehlsen Associates to pursue future exploration of multi-DoF WEC designs.

The modeling and control work in this project began with integration of pitch kinematics and angular momentum into a single pod, state space plant model. A second disturbance vector for pitch excitation was then introduced, allowing for heave-only MPC control with the new 2 DoF state space model. Direct pitch control was then added to the MPC formulation and used to evaluate the heave-pitch controller with linear and non-linear hydrodynamics using 2 DoF MPC and the WEC-Sim model.

The power gain resulting from this project fell within the mean power improvement range anticipated. In moving from 1-DoF (heave) to 2-DoF (heave-pitch), the power gain for a single pod is 13.7% for both the linear and nonlinear hydro results, providing a justification for further pursuit of this line of research and continued work to integrate this DoF with the larger WEC

1 INTRODUCTION TO THE PROJECT

The "Centipod" wave energy converter's (WEC) main potential design limitation is the inherent theoretical capture limit of a single degree of freedom (DoF) heaving point absorber. As stated by Uaine Gorm and the European Marine Energy Center in a recent design assessment of Centipod: *"It is well established that WECs with asymmetric radiation, which is inherent in WECs that resist in surge or pitch, have greater capture potential. Point absorber capture width limits for pure surge and pure pitch are both λ/π, whilst combined modes of heave/pitch or surge/pitch fare even better at 3λ/2π."*

Dehlsen Associates has already developed a mechanical means of accomplishing this second, pitch DOF and already possess a functional, validated numerical model with coupled model predictive control (MPC). Therefore, the only missing component is the technical know-how to implement a second DOF in the MPC optimization formulation. This is well within the demonstrated technical capability of the OSU team and upon hand-off of the updated control formulation, the value of this work will be immediately evaluated as a quantitative impact with Dehlsen Associates' in-house capabilities.

2 ROLES AND RESPONSIBILITIES OF PROJECT PARTICIPANTS

Oregon State University Wallace Energy Systems & Renewables Facility (OSU WESRF) will provide the main body of work in this project. Meanwhile, the applicant, Dehlsen Associates, will provide guidance and system integration with their WEC's numerical model.

2.1 APPLICANT RESPONSIBILITIES AND TASKS PERFORMED

The applicant (Dehlsen Associates) will provide data to the Network Facility (OSU) relevant to the WEC, enabling initiation of their work scope. Near the end of the project, Dehlsen Associates will couple the resulting controller with their in-house WEC-Sim model for final testing.

2.2 NETWORK FACILITY RESPONSIBILITIES AND TASKS PERFORMED

The Network Facility (OSU) will undertake control formulation design and implementation incorporating the second degree of freedom described in Section 1.

3 PROJECT OBJECTIVES

Dehlsen Associates aims to extend its "Centipod" WEC model predictive control (MPC) algorithm from single degree of freedom (DoF) heave operation to a two degree of freedom heave-pitch control optimization. Dehlsen Associates is seeking support from OSU to expand the existing single DOF MPC

algorithm as they have played an integral role in the development of the existing single DOF MPC algorithm over the last several years[1], leaving this scope as a natural extension of prior research.

It is expected that this second DoF has the potential to provide a significant uplift in AEP just as the original single DoF MPC implementation accomplished, which resulted in a theoretical 500% improvement in AEP or a 160% improvement if conservative practical constraints were applied. Since MPC is already implemented, and will serve as the new baseline, an expected AEP increase of 10-40% is seen to be possible without constraints.

4 Test Facility, Equipment, Software, and Technical Expertise

The WESRF at OSU provides research, testing and consulting services related to motors, generators, adjustable speed drives, power electronics, power supplies, power quality, industrial process equipment, power systems and renewables.

This project, however, is focused on controls development only and will not require any physical hardware, with the exception of computers and software licenses. The software required will be MathWorks's MATLAB and Simulink[2] in addition to the open source optimal control solver ACADO[3].

5 Test or Analysis Article Description

This project is numerical only, and no test article will exist. The modeled WEC is therefore described here for context.

The Centipod WEC is comprised of multiple point-absorber buoys which heave with passing waves. These point-absorber buoys, called "Pods", react against a submerged, stable, common platform called the "Backbone", allowing for power extraction through a power take-off system between the Pods and Backbone.

The specific baseline design variant of the Centipod WEC used in this project consists of three axisymmetric Pods which have 1 degree of freedom in the heave direction. The Pods are

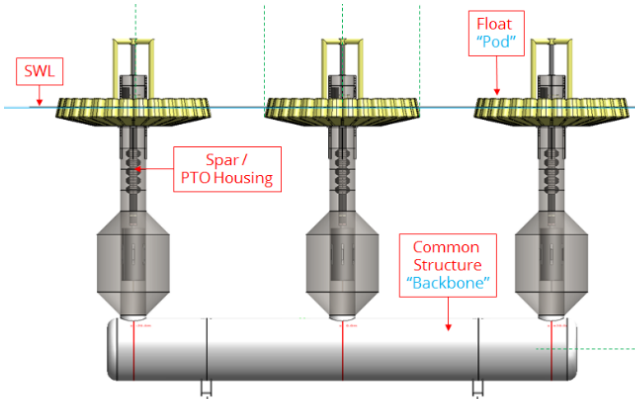

Figure a. Centipod WEC

1 M. Starrett, R. So, T. K. A. Brekken and A. McCall, "Increasing power capture from multibody wave energy conversion systems using model predictive control," 2015 IEEE Conference on Technologies for Sustainability (SusTech), Ogden, UT, 2015, pp. 20-26, doi: 10.1109/SusTech.2015.7314316.

2 "Simulink - Simulation and Model-Based Design - MATLAB & Simulink." https://www.mathworks.com/products/simulink.html (accessed Oct. 10, 2020).

3 "ACADO Toolkit." https://acado.github.io/ (accessed Oct. 10, 2020).

connected, via a spar which also houses the power take-off unit, to a tension leg moored common Backbone that provides pre-tension to the mooring lines.

6 Work Plan

The workplan will be comprised of a kick-off where WEC parameters are established between Dehlsen Associates and OSU, the main body of controls development work, and finally a hand-off and AEP impact assessment.

6.1 Experimental Setup, Data Acquisition System, and Instrumentation

Numerical Project Only – Section Not Applicable.

6.2 Numerical Model Description

The primary model used in the execution of this project will be a state-space model of the Centipod WEC to be used as a plant model and a simple model for the purposes of controller development. This state-space model was originally developed by Dehlsen Associates and OSU for the original MPC development[4] and improved over the last several years.

Once the controller is re-formulated and deemed to be complete, it will be coupled with the exiting WEC numerical model for impact assessment. The Dehlsen Associates team worked with NREL and Sandia to produce a numerical model of Centipod in WEC-Sim. The WEC-Sim model employed by the Centipod development program has subsequently been validated against CFD models and wave basin experimental data by NREL, with their conclusion being:

"*The differences between the experimental and WEC-Sim derived power and loads are well within the expected limitations of linear-based modeling and experimental error. Given these results, the Centipod WEC-Sim model has been validated, and could foreseeably be used, along with standard safety factors, to design and simulate the Centipod's power production, operational design loads, and fatigue life.*"

6.3 Test and Analysis Matrix and Schedule

The modeling and control work in this project will take place over approximately two weeks.

Week 1:

1) Integrate pitch kinematics and angular momentum into a single pod, state space plant model. The model will then be 2 DOF: heave and pitch.
2) Introduce second disturbance vector for pitch excitation.
3) Evaluate heave-only MPC controller with new 2 DOF state space model.

4 M. Starrett, R. So, T. K. A. Brekken, and A. McCall, "Development of a state space model for wave energy conversion systems," in *IEEE Power and Energy Society General Meeting*, 2015, vol. 2015-Septe, doi: 10.1109/PESGM.2015.7285998.

Week 2:

4) Add direct pitch control to MPC formulation. The MPC formulation will now be two control inputs: PTO force in heave and PTO force (torque) in pitch.

5) Evaluate the heave-pitch controller with linear hydrodynamics using 2 DOF MPC and the state space model.

Week 3:

6) Couple controller with WEC-Sim model.

7) Evaluate controller with and without non-linear hydrodynamics enabled in WEC-Sim.

6.4 Safety

Numerical Project Only – Section Not Applicable.

6.5 Contingency Plans

This is a relatively low-risk project, with the only risk being unsuccessful implementation of the control, which would likely be due to a lack of convergence in the optimal control solver. However, results indicating non-viable control will also be a valuable outcome to this project, as they will highlight needs for future research in the field of wave energy converter control.

6.6 Data Management, Processing, and Analysis

6.6.1 Data Management

Data will be stored where it is generated, whether at OSU WESRF or Dehlsen Associates, with the exception of data that is required for inter-entity exploitation of the project, which will be stored with both entities. Raw data output from MATLAB will generally be discarded, as it may be repeatably generated with the output control formulation and numerical tools. Processed outputs relevant to the evaluation of the research conducted will be saved and made available for usage in reports and direct data submissions to MHK DR.

The following will be uploaded to MHK DR:

Example Time Series (baseline 1DOF) - normalized	MATLAB data structure (.m)
Example Time Series (resultant 2DOF) - normalized	MATLAB data structure (.m)

6.6.2 Data Processing

This control formulation and numerical modeling project will not require intensive data processing as may be required for a project based on physical testing and sensor data. Some data processing will be required however to package data for useful dissemination. If the native controller and/or simulation variable names are non-intuitive for persons not involved with the project they may be renamed and

combined into a structure. For example, a variable named '*dz*' in the simulation may be packed into a test case specific structure with an intuitive name such as '*testCase01.heaveVelocity*'. If the variable or field names are non-intuitive, an explanatory memo will accompany the uploaded data.

6.6.3 Data Analysis

Data will be directly generated from the MATLAB simulations. No scaling will be required. No statistical processing will be required, unless useful for enhanced understanding of a time-series dataset. Plots will be generated where an understanding of forces or kinematics would be ideally communicated through visual means for reporting purposes.

7 PROJECT OUTCOMES

7.1 RESULTS

7.1.1. Nomenclature

v_i	Velocity (linear or angular) in i^{th} DoF.
x_i	Displacement (linear or angular) in i^{th} DoF.
ξ_i	i^{th} state variable for radiation force state-space approximation.
$F_{r,pq}$	Radiation force in p^{th} DoF due to velocity in q^{th} DoF.
$F_{hs,i}$	Hydrostatic force in i^{th} DoF.
$F_{v,i}$	Viscous drag force in i^{th}DoF.
$F_{e,i}$	Wave excitation force in i^{th}DoF.
$F_{p,i}$	PTO force in i^{th}DoF.
m	Mass of the float.
$A_{pq,\infty}$	Added mass at infinite frequency in p^{th} DoF due to acceleration in q^{th} DoF.
C_i	The hydrostatic restoring coefficient in i^{th} DoF.
$C_{vd,i}$	Viscous drag coefficient in i^{th} DoF.
A_{qp}	Frequency-dependent added mass in p^{th} DoF due to acceleration in q^{th} DoF.
B_{qp}	Frequency-dependent damping in p^{th} DoF due to velocity in q^{th} DoF.
K_{pq}	Radiation force impulse response without infinite frequency added mass.
Z_{qp}	WEC intrinsic impedance response in p^{th} DoF due to velocity in q^{th} DoF.
a_i	Polynomial coefficients.

$c_{i,j}$	Polynomial coefficients for cost functional.
$\mathbf{w}$	Set of design variables.
N	Prediction horizon.
$\rho_{N,i}$	Finite horizon terminal cost penalty.
P_i	Polynomial of design variables.
$\mathbf{\Psi_i}$	Constant matrices.
$\mathbf{B_i}$	Constant column vectors.
$\Upsilon_\mathbf{i}$	Column vectors of non-linear functions.
$\mathbf{q}$	Column vectors of non-linear functions.
$\mathbf{p}$	Column vectors of non-linear functions.
$\mathbf{u}$	Control input vector, $\mathbf{F_p}(N)$.
$\mathbf{d}$	Excitation force disturbance vector, $\mathbf{F_e}$ (N).
R_i	Some real number
$\mathbf{X} \subseteq \mathbf{w}$	State vector.
$\mathbf{u} \subseteq \mathbf{w}$	Manipulated variable.

7.1.2. Time Domain Model of a Multiple Degree of Freedom WEC

We will follow the subscript notation of WEC-Sim Toolbox [1] for the degrees of freedom for WEC, in which the integers from 1,2,.. 6 correspond to surge, sway, heave, roll, pitch, and yaw, respectively. The WEC device is a full-scale version of the Dehlsen Associates, LLC multi-pod CENTIPOD [2]. A 1:35-scale version of the device is shown in Figure 1. This CENTIPOD device has three floating pods and three spars fixed to a backbone structure, and the backbone is anchored using mooring lines, as shown in Figure 2. In its 2-DoF version, each pod is attached to a PTO mechanism in the heave and pitch DoFs. Each pod in Figure 2 is modeling as a wave point absorber device. The Cummins equation for the coupled surge and pitch dynamics for a point absorber pod (assuming a local reference frame) is given by,

$$\big(m + A_{11}(\infty)\big)\dot{v}_1 + A_{15}(\infty)\dot{v}_5 = -F_{r,11}(t) - F_{r,15}(t) - F_{v,1}(t) + F_{e,1}(t), \tag{1a}$$

$$\big(m + A_{55}(\infty)\big)\dot{v}_5 + A_{51}(\infty)\dot{v}_1 = -F_{r,55}(t) - F_{r,51}(t) - F_{v,5}(t) - F_{hs,5}(t) - F_{p,5}(t) + F_{e,5}(t). \tag{1b}$$

The Cummins equation for the heave dynamics of a point absorber pod is given by,

$$\big(m + A_{33}(\infty)\big)\dot{v}_3(t) = -F_{r,33}(t) - F_{hs,3}(t) - F_{v,3}(t) - F_{p,3}(t) + F_{e,3}(t). \tag{2}$$

The hydrostatic, viscous damping, and radiation force terms in (1) and (2) are given by,

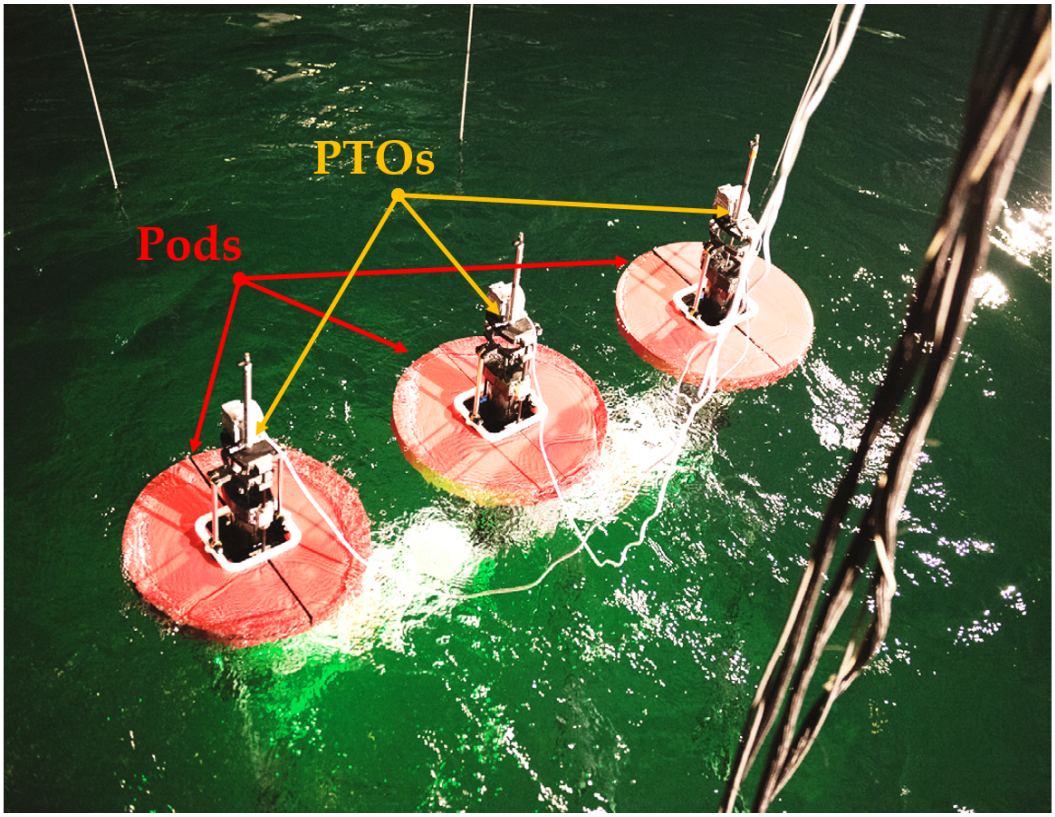

Figure 1. Image of the Dehlsen Associates, LLC, 1:35-scale CENTIPOD WEC.

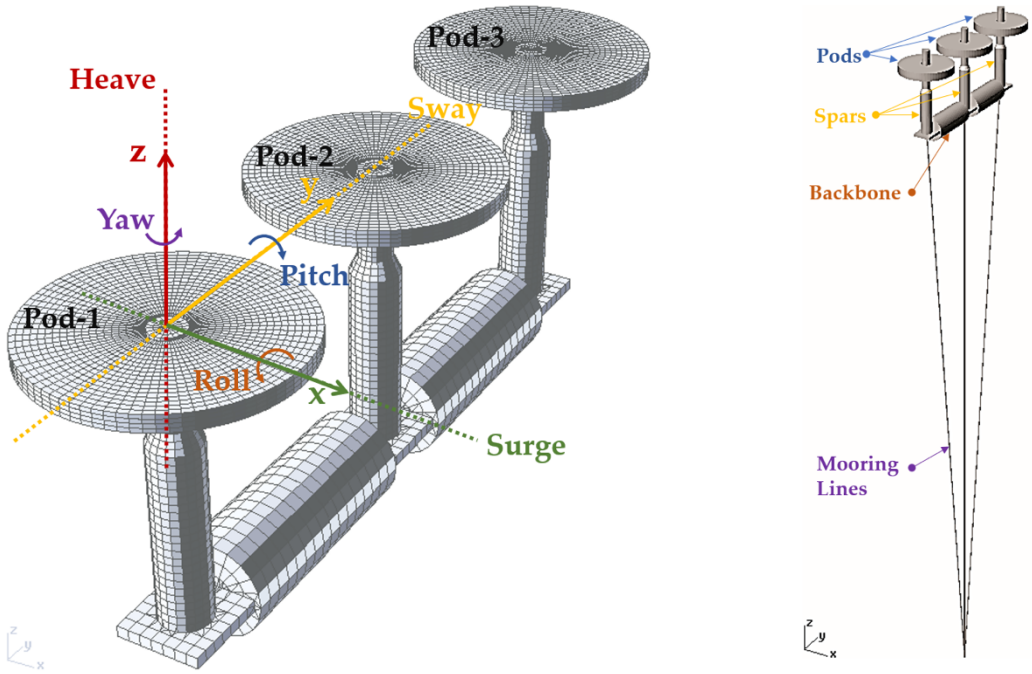

(a) (b)

Figure 2. Degrees of freedom for dynamic modeling of CENTIPOD WEC: (a) baseline configuration; (b) model with mooring lines.

$$F_{r,11}(t) = \int_{-\infty}^{t} K_{11}(t-\tau)v_1 d\tau, \tag{3a}$$

$$F_{r,15}(t) = \int_{-\infty}^{t} K_{15}(t-\tau)v_5 d\tau, \tag{3b}$$

$$F_{r,55}(t) = \int_{-\infty}^{t} K_{55}(t-\tau)v_5 d\tau, \tag{3c}$$

$$F_{r,51}(t) = \int_{-\infty}^{t} K_{51}(t-\tau)v_1 d\tau, \tag{3d}$$

$$F_{r,33}(t) = \int_{-\infty}^{t} K_{33}(t-\tau)v_3 d\tau \tag{3e}$$

$$F_{hs,i}(t) = C_i x_i, \qquad i = 3,5. \tag{3f}$$

$$F_{v,i}(t) = C_{d,i} v_i |v_i|, \qquad i = 1,3,5. \tag{3g}$$

7.1.2.1 State-Space Approximation of Radiation Force

The convolution integral term in (3a) through (3d) can be approximated by a transfer function expression,

$$F_{r,pq}(t) = \int_{-\infty}^{t} K_{pq}(t-\tau)v_q d\tau \Leftrightarrow F_{r,pq}(j\omega) = Z_{pq}(j\omega)V_q(j\omega), \tag{4}$$

Using the device data from WAMIT [3], we can approximate the intrinsic impedance $Z_{pq}(j\omega)$ in (4) by a second order transfer function using System Identification techniques,

$$Z_{pq}(j\omega) = \left[j\omega\left(A_{pq}(j\omega) - A_{pq}(\infty)\right) + B_{qp}(j\omega)\right] \approx \left.\frac{\alpha_{pq,1}s + \alpha_{pq,0}}{s^2 + \beta_{pq,1}s + \beta_{pq,0}}\right|_{s=j\omega}, \tag{5}$$

Using (5) in (4) enables us to express the radiation force as a second-order transfer function,

$$F_{r,pq}(s) \approx \frac{\alpha_{pq,1}s + \alpha_{pq,0}}{s^2 + \beta_{pq,1}s + \beta_{pq,0}} V_q(s), \tag{6}$$

The transfer function expression in (6) can be converted to the State-Space expressions in the Observer-Canonical forms for each of the radiation force term,

$$\begin{bmatrix} \dot{\xi}_k(t) \\ \dot{\xi}_{k+1}(t) \end{bmatrix} = \begin{bmatrix} 0 & 1 \\ a_k & a_{k+1} \end{bmatrix} \begin{bmatrix} \xi_k(t) \\ \xi_{k+1}(t) \end{bmatrix} + \begin{bmatrix} b_k \\ b_{k+1} \end{bmatrix} v_q(t), \tag{7a}$$

$$y_{pq}(t) = \begin{bmatrix} 1 & 0 \end{bmatrix} \begin{bmatrix} \xi_k(t) \\ \xi_{k+1}(t) \end{bmatrix} \approx F_{r,pq}(t). \tag{7b}$$

by the comparison of (6) and (7), we have, $\alpha_{pq,1} = b_k$, $\beta_{pq,1} = -a_{k+1}, \beta_{pq,0} = -a_k$, and $\alpha_{pq,0} = b_{k+1} - b_k a_{k+1}$.

7.1.2.2 State-Space Description of Surge-Pitch Dynamics

Making a change of variables in (1),

$$M_{ii} = \left(m + A_{ii}(\infty)\right), \qquad i = 1,3,5 \tag{8a}$$

$$F_{1,net} = -F_{r,11}(t) - F_{r,15}(t) - F_{v,1}(t) + F_{e,1}(t), \tag{8b}$$

$$F_{5,net} = -F_{r,55}(t) - F_{r,51}(t) - C_5 x_5 - F_{v,5}(t) - F_{p,5}(t) + F_{e,5}(t). \tag{8c}$$

Using (8) in (1), we get the pitch-surge coupled model of a pod as,

$$\begin{bmatrix} M_{11} & A_{15}(\infty) \\ A_{51}(\infty) & M_{55} \end{bmatrix} \begin{bmatrix} \dot{v}_1 \\ \dot{v}_5 \end{bmatrix} = \begin{bmatrix} F_{1,net} \\ F_{5,net} \end{bmatrix} \tag{9a}$$

$$\begin{bmatrix} \dot{v}_1 \\ \dot{v}_5 \end{bmatrix} = \begin{bmatrix} m_{11} & m_{15} \\ m_{51} & m_{55} \end{bmatrix} \begin{bmatrix} F_{1,net} \\ F_{5,net} \end{bmatrix} \tag{9b}$$

Using Equation (8) and Equation (9a), we can convert Equation (9b) into the state-space form,

$$\begin{aligned} \dot{v}_1(t) = {} & m_{11}\left(-F_{r,11}(t) - F_{r,15}(t) - F_{v,1}(t) + F_{e,1}(t)\right) \\ & + m_{15}\left(-F_{r,55}(t) - F_{r,51}(t) - C_5 x_5 - F_{v,5}(t) - F_{p,5}(t) + F_{e,5}(t)\right) \end{aligned} \tag{10a}$$

$$\begin{aligned} \dot{v}_5(t) = {} & m_{51}\left(-F_{r,11}(t) - F_{r,15}(t) - F_{v,1}(t) + F_{e,1}(t)\right) \\ & + m_{55}\left(-F_{r,55}(t) - F_{r,51}(t) - C_5 x_5 - F_{v,5}(t) - F_{p,5}(t) + F_{e,5}(t)\right) \end{aligned} \tag{10b}$$

Where following the (7) for each radiation force term in (10),

$$F_{r,11}(t) \approx \xi_3(t) \Leftrightarrow \begin{bmatrix} \dot{\xi}_3(t) \\ \dot{\xi}_4(t) \end{bmatrix} = \begin{bmatrix} 0 & 1 \\ a_3 & a_4 \end{bmatrix} \begin{bmatrix} \xi_3(t) \\ \xi_4(t) \end{bmatrix} + \begin{bmatrix} b_3 \\ b_4 \end{bmatrix} v_1(t) \tag{11a}$$

$$F_{r,15}(t) \approx \xi_5(t) \Leftrightarrow \begin{bmatrix} \dot{\xi}_5(t) \\ \dot{\xi}_6(t) \end{bmatrix} = \begin{bmatrix} 0 & 1 \\ a_5 & a_6 \end{bmatrix} \begin{bmatrix} \xi_5(t) \\ \xi_6(t) \end{bmatrix} + \begin{bmatrix} b_5 \\ b_6 \end{bmatrix} v_5(t) \tag{11b}$$

$$F_{r,55}(t) \approx \xi_7(t) \Leftrightarrow \begin{bmatrix} \dot{\xi}_7(t) \\ \dot{\xi}_8(t) \end{bmatrix} = \begin{bmatrix} 0 & 1 \\ a_7 & a_8 \end{bmatrix} \begin{bmatrix} \xi_7(t) \\ \xi_8(t) \end{bmatrix} + \begin{bmatrix} b_7 \\ b_8 \end{bmatrix} v_5(t) \tag{11c}$$

$$F_{r,51}(t) \approx \xi_9(t) \Leftrightarrow \begin{bmatrix} \dot{\xi}_9(t) \\ \dot{\xi}_{10}(t) \end{bmatrix} = \begin{bmatrix} 0 & 1 \\ a_9 & a_{10} \end{bmatrix} \begin{bmatrix} \xi_9(t) \\ \xi_{10}(t) \end{bmatrix} + \begin{bmatrix} b_9 \\ b_{10} \end{bmatrix} v_1(t) \tag{11d}$$

Using variables from (11) in (10), we get,

$$\begin{aligned} \dot{v}_1(t) = {} & m_{11}\left(-\xi_3(t) - \xi_5(t) - F_{v,1}(t) + F_{e,1}(t)\right) \\ & + m_{15}\left(-\xi_7(t) - \xi_9(t) - C_5 x_5 - F_{v,5}(t) - F_{p,5}(t) + F_{e,5}(t)\right) \end{aligned} \tag{12a}$$

$$\begin{aligned} \dot{v}_5(t) = {} & m_{51}\left(-\xi_3(t) - \xi_5(t) - F_{v,1}(t) + F_{e,1}(t)\right) \\ & + m_{55}\left(-\xi_7(t) - \xi_9(t) - C_5 x_5 - F_{v,5}(t) - F_{p,5}(t) + F_{e,5}(t)\right) \end{aligned} \tag{12b}$$

Expanding (12) we get,

$$\dot{v}_1(t) = -m_{15}C_5x_5 - m_{11}\xi_3(t) - m_{11}\xi_5(t) - m_{15}\xi_7(t) - m_{15}\xi_9(t) - m_{11}F_{v,1}(t) - m_{15}F_{v,5}(t) - m_{15}F_{p,5}(t) + m_{11}F_{e,1}(t) + m_{15}F_{e,5}(t) \tag{13a}$$

$$\dot{v}_5(t) = -m_{55}C_5x_5 - m_{51}\xi_3(t) - m_{51}\xi_5(t) - m_{55}\xi_7(t) - m_{55}\xi_9(t) - m_{55}F_{v,5}(t) - m_{51}F_{v,1}(t) - m_{55}F_{p,5}(t) + m_{51}F_{e,1}(t) + m_{55}F_{e,5}(t) \tag{13c}$$

$$\dot{x}_5(t) = v_5(t) \tag{13d}$$

We can combine Equation (11) and Equation (13) to get a matrix form of the surge-pitch state-space model,

$$\begin{bmatrix} \dot{v}_1 \\ \dot{v}_5 \\ \dot{x}_5 \\ \dot{\xi}_3 \\ \dot{\xi}_4 \\ \dot{\xi}_5 \\ \dot{\xi}_6 \\ \dot{\xi}_7 \\ \dot{\xi}_8 \\ \dot{\xi}_9 \\ \dot{\xi}_{10} \end{bmatrix}_{11\times1} = \begin{bmatrix} 0 & 0 & -m_{15}C_5 & -m_{11} & 0 & -m_{11} & 0 & -m_{15} & 0 & -m_{15} & 0 \\ 0 & 0 & -m_{55}C_5 & -m_{51} & 0 & -m_{51} & 0 & -m_{55} & 0 & -m_{55} & 0 \\ 0 & 1 & 0 & 0 & 0 & 0 & 0 & 0 & 0 & 0 & 0 \\ b_3 & 0 & 0 & 0 & 1 & 0 & 0 & 0 & 0 & 0 & 0 \\ b_4 & 0 & 0 & a_3 & a_4 & 0 & 0 & 0 & 0 & 0 & 0 \\ 0 & b_5 & 0 & 0 & 0 & 0 & 1 & 0 & 0 & 0 & 0 \\ 0 & b_6 & 0 & 0 & 0 & a_5 & a_6 & 0 & 0 & 0 & 0 \\ 0 & b_7 & 0 & 0 & 0 & 0 & 0 & 0 & 1 & 0 & 0 \\ 0 & b_8 & 0 & 0 & 0 & 0 & 0 & a_7 & a_8 & 0 & 0 \\ b_9 & 0 & 0 & 0 & 0 & 0 & 0 & 0 & 0 & 0 & 1 \\ b_{10} & 0 & 0 & 0 & 0 & 0 & 0 & 0 & 0 & a_9 & a_{10} \end{bmatrix} \begin{bmatrix} v_1 \\ v_5 \\ x_5 \\ \xi_3 \\ \xi_4 \\ \xi_5 \\ \xi_6 \\ \xi_7 \\ \xi_8 \\ \xi_9 \\ \xi_{10} \end{bmatrix} + \begin{bmatrix} -m_{11} & -m_{15} \\ -m_{51} & -m_{55} \\ 0 & 0 \\ 0 & 0 \\ 0 & 0 \\ 0 & 0 \\ 0 & 0 \\ 0 & 0 \\ 0 & 0 \\ 0 & 0 \\ 0 & 0 \end{bmatrix} \begin{bmatrix} F_{v,1} \\ F_{v,5} \end{bmatrix} + \begin{bmatrix} -m_{15} \\ -m_{55} \\ 0 \\ 0 \\ 0 \\ 0 \\ 0 \\ 0 \\ 0 \\ 0 \\ 0 \end{bmatrix} F_{p,5} + \begin{bmatrix} m_{11} & m_{15} \\ m_{51} & m_{55} \\ 0 & 0 \\ 0 & 0 \\ 0 & 0 \\ 0 & 0 \\ 0 & 0 \\ 0 & 0 \\ 0 & 0 \\ 0 & 0 \\ 0 & 0 \end{bmatrix} \begin{bmatrix} F_{e,1} \\ F_{e,5} \end{bmatrix} \tag{14}$$

7.1.2.3. State-Space Description of Heave Dynamics

The radiation force term in (3) for heave axis can be expressed by following state-space description by using (3e), (6), and (7),

$$F_{r,33}(t) \approx \xi_1(t) \Leftrightarrow \begin{bmatrix} \dot{\xi}_1(t) \\ \dot{\xi}_2(t) \end{bmatrix} = \begin{bmatrix} 0 & 1 \\ a_1 & a_2 \end{bmatrix} \begin{bmatrix} \xi_1(t) \\ \xi_2(t) \end{bmatrix} + \begin{bmatrix} b_1 \\ b_2 \end{bmatrix} v_3(t) \tag{15}$$

Using (15) with $M_{33} = m + A_{33}(\infty)$, we can convert (1) into a state-space form as,

$$\dot{v}_3(t) = \frac{1}{M_{33}}\left(-\xi_1(t) - C_3x_3(t) - F_{v,3}(t) - F_{p,3}(t) + F_{e,3}(t)\right) \tag{16a}$$

$$\dot{x}_3(t) = v_3(t) \tag{16b}$$

Combining (15) and (16), we get the final expression for the heave dynamics in the state-space matrix form,

$$\begin{bmatrix} \dot{v}_3 \\ \dot{x}_3 \\ \dot{\xi}_1 \\ \dot{\xi}_2 \end{bmatrix} = \begin{bmatrix} 0 & \frac{-C_3}{M_{33}} & \frac{-1}{M_{33}} & 0 \\ 1 & 0 & 0 & 0 \\ b_1 & 0 & 0 & 1 \\ b_2 & 0 & a_1 & a_2 \end{bmatrix} \begin{bmatrix} v_3 \\ x_3 \\ \xi_1 \\ \xi_1 \end{bmatrix} + \begin{bmatrix} \frac{-1}{M_{33}} \\ 0 \\ 0 \\ 0 \end{bmatrix} F_{v,3}(t) + \begin{bmatrix} \frac{-1}{M_{33}} \\ 0 \\ 0 \\ 0 \end{bmatrix} F_{p,3}(t) + \begin{bmatrix} \frac{1}{M_{33}} \\ 0 \\ 0 \\ 0 \end{bmatrix} F_{e,3}(t) \tag{17}$$

7.1.2.4. Combined Surge-Pitch-Heave State-Space Model

We can combine the coupled surge-pitch dynamics in (14) with heave dynamics in (17) to get a combined Surge-Pitch-Heave model,

$$\dot{\mathbf{X}} = \mathbf{A}\mathbf{X} + \mathbf{B_v}\mathbf{F_v} + \mathbf{B_p}\mathbf{F_p} + \mathbf{B_e}\mathbf{F_e} \tag{18}$$

where

$$\mathbf{F_p} = [F_{p,5} \quad F_{p,3}]^T \tag{19a}$$

$$\mathbf{F_v} = [F_{v,1} \quad F_{v,5} \quad F_{v,3}]^T \tag{19b}$$

$$\mathbf{F_e} = [F_{e,1} \quad F_{e,5} \quad F_{e,3}]^T \tag{19c}$$

$$\mathbf{X} = [v_1 \quad v_5 \quad x_5 \quad \xi_3 \quad \xi_4 \quad \xi_5 \quad \xi_6 \quad \xi_7 \quad \xi_8 \quad \xi_9 \quad \xi_{10} \quad v_3 \quad x_3 \quad \xi_1 \quad \xi_2]^T \tag{19d}$$

The radiation force terms are approximated by following state variables using (7),

$$F_{r,11} = \xi_3,\ F_{r,15} = \xi_5,\ F_{r,51} = \xi_7,\ F_{r,55} = \xi_9,\ F_{r,33} = \xi_1 \tag{20}$$

The state-space matrices in (18) are developed in (21).

7.1.2.5. Polynomial Approximations of Quadratic Viscous Drag Force

The quadratic viscous drag term $v_i|v_i|$ in (3g) makes the overall WEC dynamic problem numerically 'stiff.' One solution is to approximate this term with a smooth higher-order polynomial. A third-order polynomial approximation for $v_i|v_i|$ is used in the surge and heave axis as shown in Figure 3(a), where the range of interest of velocity in m/sec is $v_i \in (-1.5, 1.5)$, and a fifth-order polynomial approximation is used for the pitch axis as shown in Figure 3(b), where the range of interest of velocity in rad/sec is $v_i \in (-0.5, 0.5)$. So, with $p_{i,j}$ being the j^{th} polynomial coefficient for i^{th} degree polynomial curve fit,

$$F_{v,i} = C_{d,i} v_i|v_i| \approx C_{d,i}\left(p_{3,3} v_i^3 + p_{3,1} v_i\right), \qquad i = 1,3. \tag{22a}$$

$$F_{v,5} = C_{d,5} v_5|v_5| \approx C_{d,5}\left(p_{5,5} v_5^5 + p_{5,3} v_5^3 + p_{5,1} v_5\right) \tag{22b}$$

$$\mathrm{A} = \begin{bmatrix} 0 & 0 & -m_{15}C_5 & -m_{11} & 0 & -m_{11} & 0 & -m_{15} & 0 & -m_{15} & 0 \\ 0 & 0 & -m_{55}C_5 & -m_{51} & 0 & -m_{51} & 0 & -m_{55} & 0 & -m_{55} & 0 \\ 0 & 1 & 0 & 0 & 0 & 0 & 0 & 0 & 0 & 0 & 0 \\ b_3 & 0 & 0 & 0 & 1 & 0 & 0 & 0 & 0 & 0 & 0 \\ b_4 & 0 & 0 & a_3 & a_4 & 0 & 0 & 0 & 0 & 0 & 0 \\ 0 & b_5 & 0 & 0 & 0 & 0 & 1 & 0 & 0 & 0 & 0 \\ 0 & b_6 & 0 & 0 & 0 & a_5 & a_6 & 0 & 0 & 0 & 0 \\ 0 & b_7 & 0 & 0 & 0 & 0 & 0 & 0 & 1 & 0 & 0 \\ 0 & b_8 & 0 & 0 & 0 & 0 & 0 & a_7 & a_8 & 0 & 0 \\ b_9 & 0 & 0 & 0 & 0 & 0 & 0 & 0 & 0 & 0 & 1 \\ b_{10} & 0 & 0 & 0 & 0 & 0 & 0 & 0 & 0 & a_9 & a_{10} \end{bmatrix} \quad \mathbf{0}_{11\times 4} \quad \mathbf{0}_{4\times 11} \quad \begin{bmatrix} 0 & \frac{-C_3}{M_{33}} & \frac{-1}{M_{33}} & 0 \\ 1 & 0 & 0 & 0 \\ b_1 & 0 & 0 & 1 \\ b_2 & 0 & a_1 & a_2 \end{bmatrix} \tag{21a}$$

$$\mathbf{B_p} = \begin{bmatrix} -m_{15} & 0 \\ -m_{55} & 0 \\ 0 & 0 \\ 0 & 0 \\ 0 & 0 \\ 0 & 0 \\ 0 & 0 \\ 0 & 0 \\ 0 & 0 \\ 0 & \frac{-1}{M_{33}} \\ 0 & 0 \\ 0 & 0 \\ 0 & 0 \end{bmatrix}, \mathbf{B_v} = \begin{bmatrix} -m_{11} & -m_{15} & 0 \\ -m_{51} & -m_{55} & 0 \\ 0 & 0 & 0 \\ 0 & 0 & 0 \\ 0 & 0 & 0 \\ 0 & 0 & 0 \\ 0 & 0 & 0 \\ 0 & 0 & 0 \\ 0 & 0 & 0 \\ 0 & 0 & 0 \\ 0 & 0 & \frac{-1}{M_{33}} \\ 0 & 0 & 0 \\ 0 & 0 & 0 \\ 0 & 0 & 0 \end{bmatrix}, \mathbf{B_e} = \begin{bmatrix} m_{11} & m_{15} & 0 \\ m_{51} & m_{55} & 0 \\ 0 & 0 & 0 \\ 0 & 0 & 0 \\ 0 & 0 & 0 \\ 0 & 0 & 0 \\ 0 & 0 & 0 \\ 0 & 0 & 0 \\ 0 & 0 & 0 \\ 0 & 0 & 0 \\ 0 & 0 & \frac{1}{M_{33}} \\ 0 & 0 & 0 \\ 0 & 0 & 0 \\ 0 & 0 & 0 \end{bmatrix} \tag{21b}$$

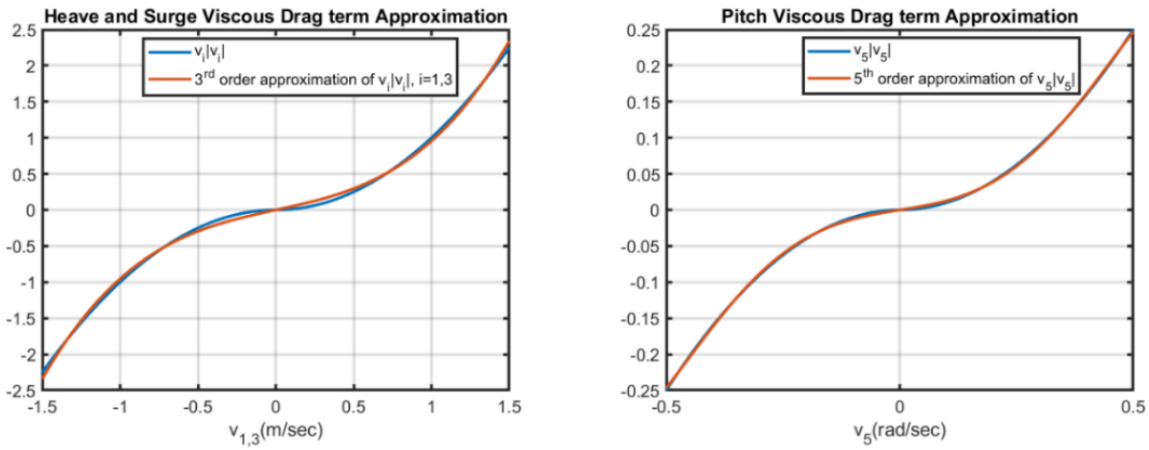

(a) (b)

Figure 3. Polynomial approximations of the quadratic drag term $v_i|v_i|$: (a) 3rd order curve fit for heave and surge axes; (b) 5th order curve fit for pitch axis.

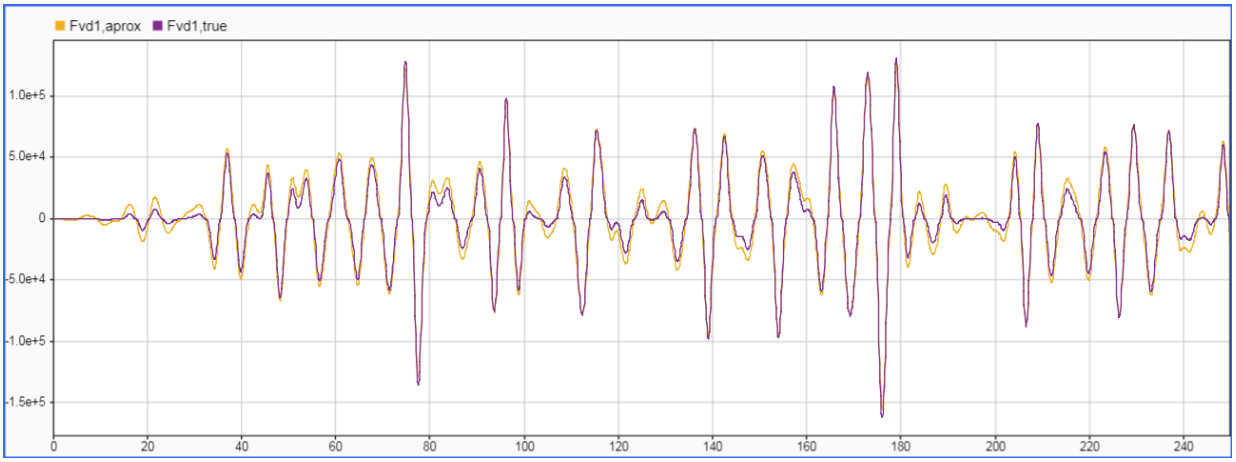

(a)

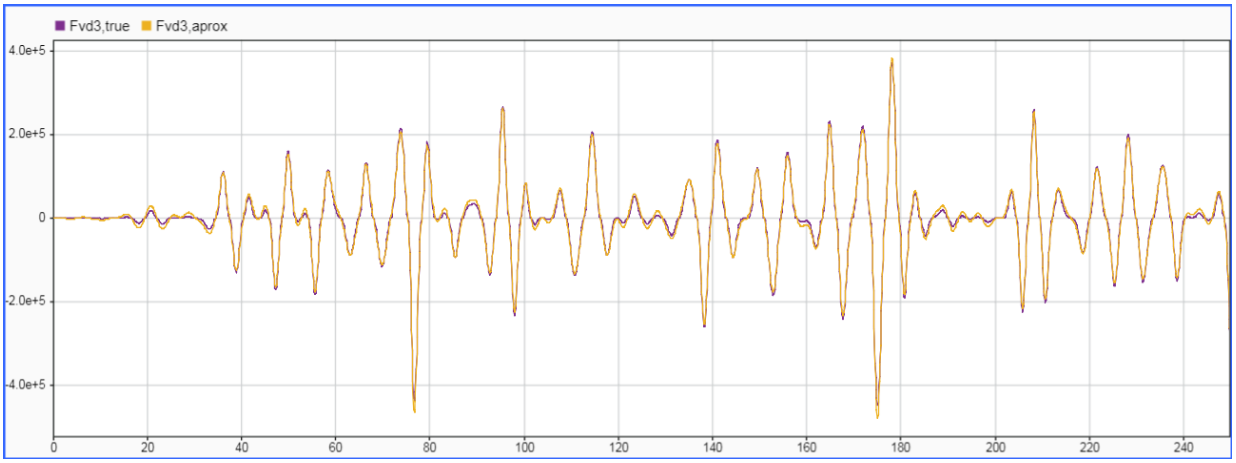

(b)

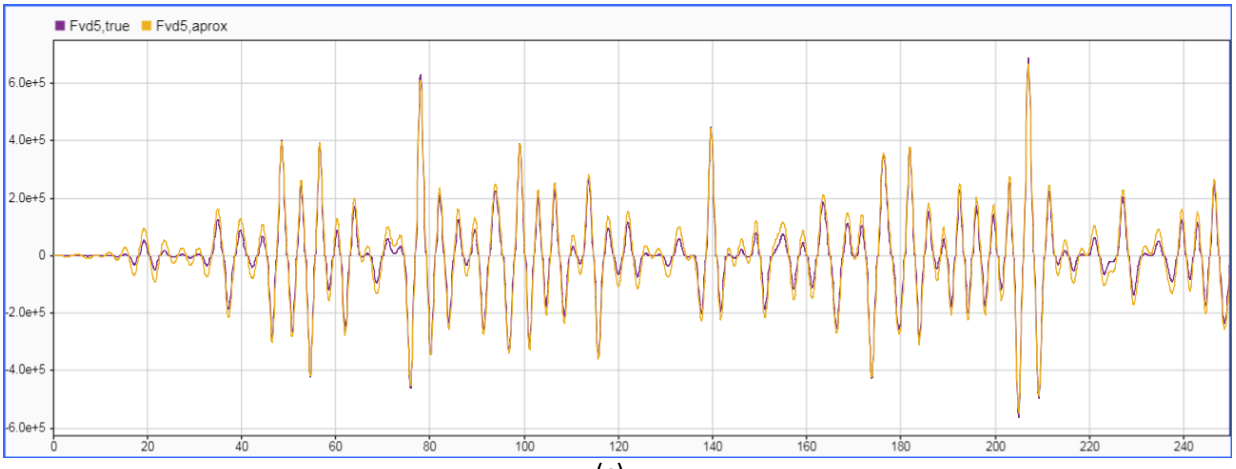

(c)

Figure 4. Polynomial approximations of the quadratic drag term $v_i|v_i|$: (a) 3[rd] order curve fit for surge; (b) 3[rd] order curve fit for heave; (c) 5[th] order curve fit for pitch axis.

7.1.2.6. Nonlinear Plant Model for NMPC

Putting (22) in (18) gives us a nonlinear 2-DoF (Heave and Pitch) WEC plant model, where the surge is coupled with the pitch and heave is a decoupled DoF. We can use this plant model as a prediction model in NMPC. We can also include the PTO currents, $I_{p,i}(F_{p,i})$, as a state in (11) to incorporate the nonlinear PTO model in the WEC model (21). We can also use the model with a differential input form, which is more friendly for optimization. This can be achieved by expressing the control variables, PTO forces, as states and considering their derivatives as inputs to the model. The resulting model format in (21) is supported in ACADO toolbox in MATLAB.

$$
\begin{aligned}
\dot{v}_1 &= m_{11}\left(-\xi_3 - \xi_5 - C_{d,1}\left(p_{13,3}v_1^3 + p_{13,1}v_1\right) + F_{e,1}\right) \\
&\quad + m_{15}\left(-C_5x_5 - \xi_7 - \xi_9 - C_{d,5}\left(p_{5,5}v_5^5 + p_{5,3}v_5^3 + p_{5,1}v_5\right) - F_{p,5} + F_{e,5}\right) \\
\dot{v}_5 &= m_{55}\left(-C_5x_5 - \xi_7 - \xi_9 - C_{d,5}\left(p_{5,5}v_5^5 + p_{5,3}v_5^3 + p_{5,1}v_5\right) - F_{p,5} + F_{e,5}\right) \\
&\quad + m_{51}\left(-\xi_3 - \xi_5 - C_{d,1}\left(p_{13,3}v_1^3 + p_{13,1}v_1\right) + F_{e,1}\right) \\
\dot{x}_5 &= v_5 \\
\dot{\xi}_3 &= b_3v_1 + \xi_4 \\
\dot{\xi}_4 &= b_4v_1 + a_3\xi_3 + a_4\xi_4 \\
\dot{\xi}_5 &= b_5v_5 + \xi_6 \\
\dot{\xi}_6 &= b_6v_5 + a_5\xi_5 + a_6\xi_6 \\
\dot{\xi}_7 &= b_7v_5 + \xi_8 \\
\dot{\xi}_8 &= b_8v_5 + a_7\xi_7 + a_8\xi_8 \\
\dot{\xi}_9 &= b_9v_1 + \xi_{10} \\
\dot{\xi}_{10} &= b_{10}v_1 + a_9\xi_9 + a_{10}\xi_{10} \\
\dot{v}_3 &= \left(1/M_{33}\right)\left(-\xi_1(t) - C_3x_3(t) - C_{d,3}\left(p_{13,3}v_3^3 + p_{13,1}v_3\right) - F_{p,3}(t) + F_{e,3}(t)\right) \\
\dot{x}_3 &= v_3 \\
\dot{\xi}_1 &= b_1v_3 + \xi_2 \\
\dot{\xi}_2 &= b_2v_3 + a_1\xi_1 + a_2\xi_2 \\
\dot{F}_{p,3} &= \frac{d}{dt}F_{p,3} = dF_{p,3} \\
\dot{F}_{p,5} &= \frac{d}{dt}F_{p,5} = dF_{p,5} \\
\dot{I}_{p,3} &= \left(\frac{dI_{p,3}}{dt}\right)\frac{d}{dt}F_{p,3} = \left(\frac{dI_{p,3}}{dt}\right)dF_{p,3} \\
\dot{I}_{p,5} &= \left(\frac{dI_{p,5}}{dt}\right)\frac{d}{d}F_{p,5} = \left(\frac{dI_{p,5}}{dt}\right)dF_{p,5}
\end{aligned}
\tag{22}
$$

7.1.2.7. Matlab Implementation of WEC State-Space Model

7.1.2.7.a Heave Model in MATLAB

The heave model in (17) is implemented in MATLAB as shown below,

```
% continuous time state space WEC model for Heave
Aplant33=[  0      -C3/M33     -1/M33       0
            1        0           0          0
            b1       0           0          1
            b2       0           a1        a2];

Bplant33=[ 1/M33     0          0         0]';
Cplant33=eye(4);
Dplant33=zeros(4,1);
```

7.1.2.7.b Surge-Pitch Model in Matlab

The surge-pitch model in (14) is implemented in MATLAB as shown below,

```
% continuous time state space WEC model for Surge and Pitch
%       1            2       3       4         5       6         7       8       9       10       11
% [     v1           v5      x5      e3(Fr11) e4     e5(Fr15) e6     e7(Fr55) e8     e9(Fr51) e10]

 A15=[  0             0     -m15*C5   -m11     0      -m11     0       -m15    0      -m15     0       %dv1
        0             0     -m55*C5   -m51     0      -m51     0       -m55    0      -m55     0       %dv5
        0             1       0         0      0        0      0         0     0        0      0       %dx5
        b3            0       0         0      1        0      0         0     0        0      0       %de3
        b4            0       0         a3     a4       0      0         0     0        0      0       %de4
        0             b5      0         0      0        0      1         0     0        0      0       %7e5
        0             b6      0         0      0        a5     a6        0     0        0      0       %8e6
        0             b7      0         0      0        0      0         0     1        0      0       %9e7
        0             b8      0         0      0        0      0         a7    a8       0      0       %10e8
        b9            0       0         0      0        0      0         0     0        0      1       %11e9
        b10           0       0         0      0        0      0         0     0        a9     a10 ]; %12e10

 B15=[  m11           m51     0         0      0        0      0         0     0        0      0
        m15           m55     0         0      0        0      0         0     0        0      0]';

 C15=eye(11);
 D15=zeros(11,2);
```

7.1.2.7.c Combined Surge-Heave-Pitch Model in MATLAB

The combined surge-heave-pitch model in (21) is implemented in MATLAB as shown below,

```
% continuous time state space WEC model with SSurge-pitch and heave
Aplant=[A15             zeros(11,4)
        zeros(4,11)     Aplant33];

Bplant=[B15             zeros(11,1)
        zeros(4,2)      Bplant33];

Cplant=[C15             zeros(11,4)
        zeros(4,11)     Cplant33];

Dplant=[D15             zeros(11,1)
        zeros(4,2)      Dplant33] ;
```

7.1.2.7.d Surge-Pitch-Heave Augmented Nonlinear Model of WEC for Embedding in the NMPC

The MATLAB implementation of (22) using ACADO toolkit is shown below. It has some extra states to include a variable number of PTO pickup coils of the linear generator.

```
%% ================> Code SECTION 3_ Surge+Heave+pitch <================
% Defining Nonlinear Plant model to be embedded in Acado NLMPC
%==> Define Variable roles
Disturbance Fe1 Fe3 Fe5;
DifferentialState v1 v5 x5 e3 e4 e5 e6 e7 e8 e9 e10 v3 x3 e1 e2 Fp3 Fp5 Ip3 Ip5 Np3 Np5;
Control dFp3 dFp5;
%==> Differential Equation Model
%    each f(i) defines the derivative of state variables, where i represent
%    the position number of states in state declaration command
%    'Differential State', i.e. x5 is third in that list so f(3) is derivative of x5.
f(1)=   m11*(-e3 -e5 -Cd1*(p133*v1^3+p131*v1) +Fe1) ...
         + m15*(-C5*x5 -e7 -e9 -Cd5*(p55*v5^5+p53*v5^3+p51*v5) -Np5*Fp5  +Fe5);
f(2)=   m55*(-C5*x5 -e7 -e9 -Cd5*(p55*v5^5+p53 *v5^3+p51 *v5) -Np5*Fp5 +Fe5)...
         + m51*(-e3 -e5 -Cd1*(p133*v1^3+p131*v1) +Fe1);
f(3)=   v5;
f(4)=   b3*v1            + e4;
f(5)=   b4*v1   +a3*e3   + a4*e4;
f(6)=   b5*v5            + e6;
f(7)=   b6*v5   +a5*e5   + a6*e6;
f(8)=   b7*v5            + e8;
f(9)=   b8*v5   +a7*e7   + a8*e8;
f(10)=  b9*v1            + e10;
f(11)=  b10*v1 +a9*e9    + a10*e10;
f(12)= (1/M33)*(-e1 -C3*x3 -Cd3*(p133*v3^3+p131*v3) -Np3*Fp3 +Fe3);
f(13)= v3;
f(14)= b1*v3             + e2;
f(15)= b2*v3  + a1*e1 + a2*e2;
f(16)= dFp3;
f(17)= dFp5;
f(18)= ((-9.0320e-13)*3*Fp3^2+(-4.4077e-24)*2*Fp3+(-0.0024))* dFp3;
f(19)= ((-9.0320e-13)*3*Fp5^2+(-4.4077e-24)*2*Fp5+(-0.0024))* dFp5;
f(20)= 0;
f(21)= 0;
%Note: Np3 and Np5 are dummy states, an indirect way of entering variable
%parameters in the model, these are number of PTO Pictup coils
```

7.1.3. Identification of Radiation Force State-Space Parameters

The radiation force state-space model parameters, a_i and b_i in (11), (15), (21), and (22) are determined by fitting a transfer function model in the data from BEMIO. For this purpose, the System-Identification GUI in Matlab has been used, as shown in Figure 5.

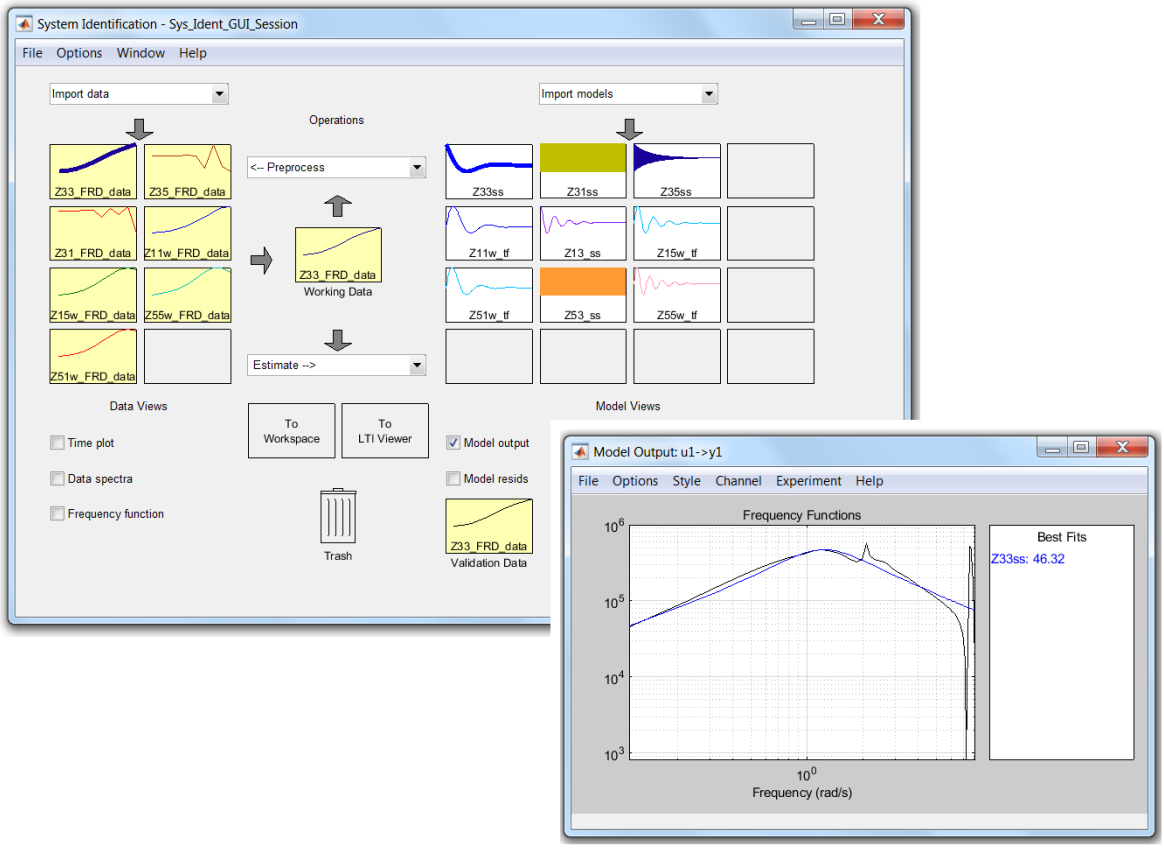

Figure 5. System Identification GUI in MATLAB and example results for $F_{r,33}$ System Identification.

7.1.3.1. $F_{r,11}$ Radiation Force State-Space Model Identification

The system identification for the frequency response data object for $F_{r,11}$ constructed from BEMIO data is shown in Figure 6. The corresponding identified state-space model in the observer-canonical form is shown in Figure 7.

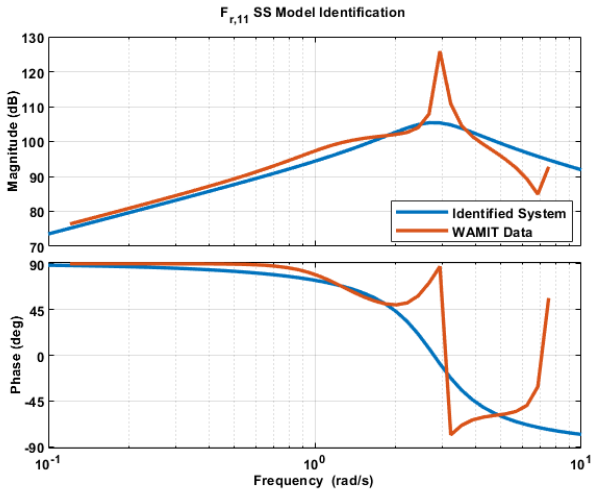

Figure 6. System Identification results, $F_{r,11}$(blue), frequency response data from BEMIO (Brown).

```
Z11tf =

  From input "u1" to output:
       4.64e05 s
  --------------------
  s^2 + 1.984 s + 7.82

Continuous-time transfer function.


Z11ss =

  A =
          x1      x2
   x1      0       1
   x2   -7.82  -1.984

  B =
              u1
   x1   3.712e+05
   x2  -7.366e+05

  C =
       x1  x2
   y1   1   0
```

Figure 7. Observer-canonical form of state-space description for $F_{r,11}$.

7.1.3.2. $F_{r,15}$ Radiation Force State-Space Model Identification

The system identification for the frequency response data object for $F_{r,15}$ constructed from BEMIO data is shown in Figure 8. The corresponding identified state-space model in the observer-canonical form is shown in Figure 9.

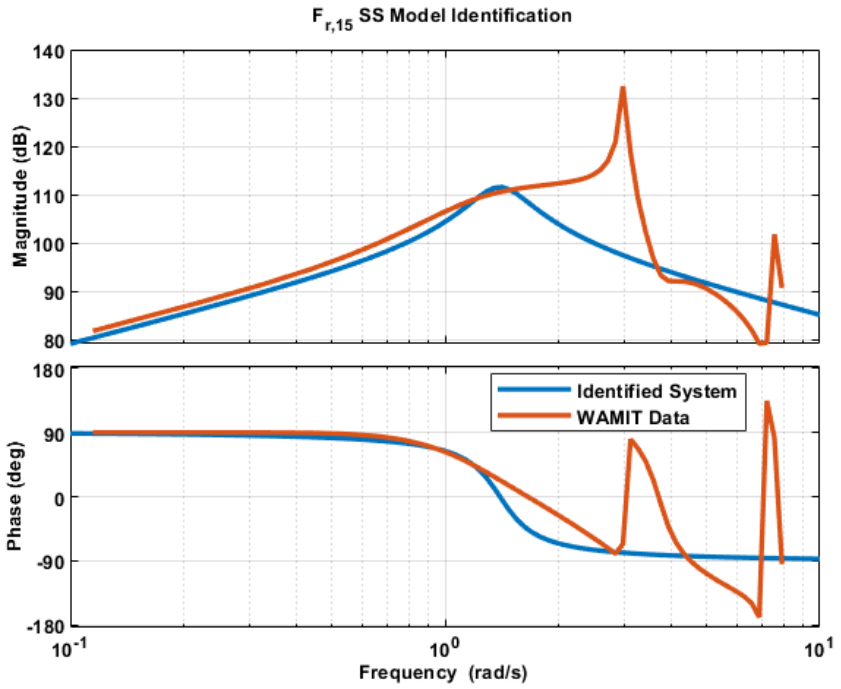

Figure 8. System Identification results, $F_{r,15}$(blue), frequency response data from BEMIO (Brown).

```
Z15tf =

  From input "u1" to output:
        2.216e05 s
  ----------------------
  s^2 + 0.4672 s + 1.962

Continuous-time transfer function.


Z15ss =

  A =
             x1        x2
   x1         0         1
   x2    -1.962   -0.4672

  B =
              u1
   x1   1.773e+05
   x2  -8.284e+04

  C =
       x1  x2
   y1   1   0
```

Figure 9. Observer-canonical form of state-space description for $F_{r,15}$.

7.1.3.3. $F_{r,55}$ Radiation Force State-Space Model Identification

The system identification for the frequency response data object for $F_{r,55}$ constructed from BEMIO data is shown in Figure 10. The corresponding identified state-space model in the observer-canonical form is shown in Figure 11.

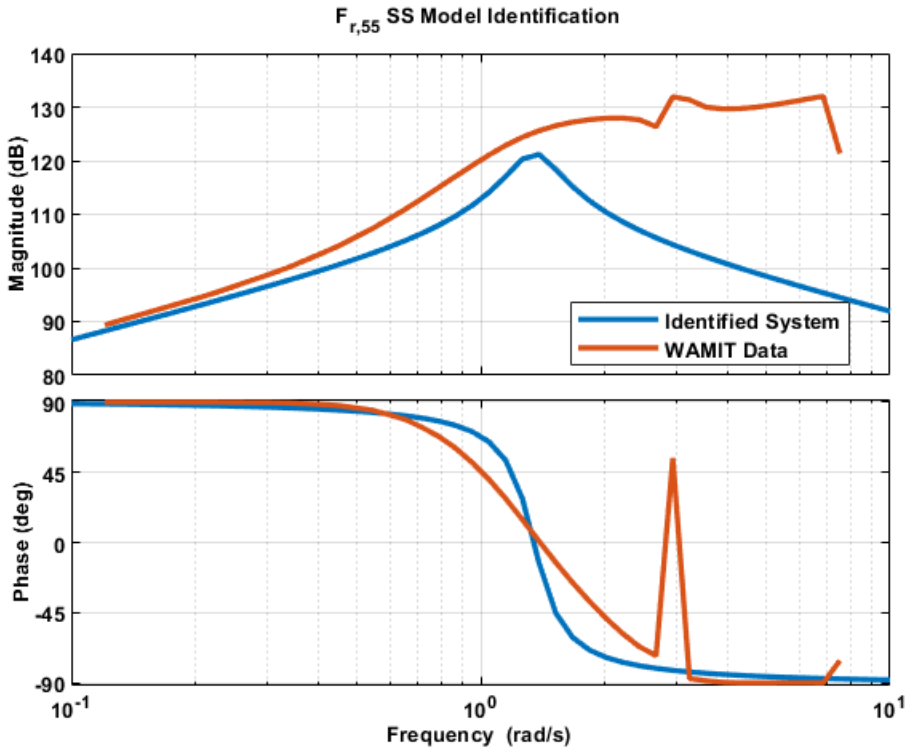

Figure 10. System Identification results, $F_{r,55}$(blue), frequency response data from BEMIO (Brown).

```
Z55tf =

  From input "u1" to output:
        4.846e05 s
  ----------------------
  s^2 + 0.3297 s + 1.822

Continuous-time transfer function.


Z55ss =

  A =
             x1       x2
   x1         0        1
   x2    -1.822  -0.3297

  B =
              u1
   x1   3.876e+05
   x2  -1.278e+05

  C =
       x1  x2
   y1   1   0
```

Figure 11. Observer-canonical form of state-space description for $F_{r,55}$.

7.1.3.4. $F_{r,51}$ Radiation Force State-Space Model Identification

The system identification for the frequency response data object for $F_{r,51}$ constructed from BEMIO data is shown in Figure 12. The corresponding identified state-space model in the observer-canonical form is shown in Figure 13.

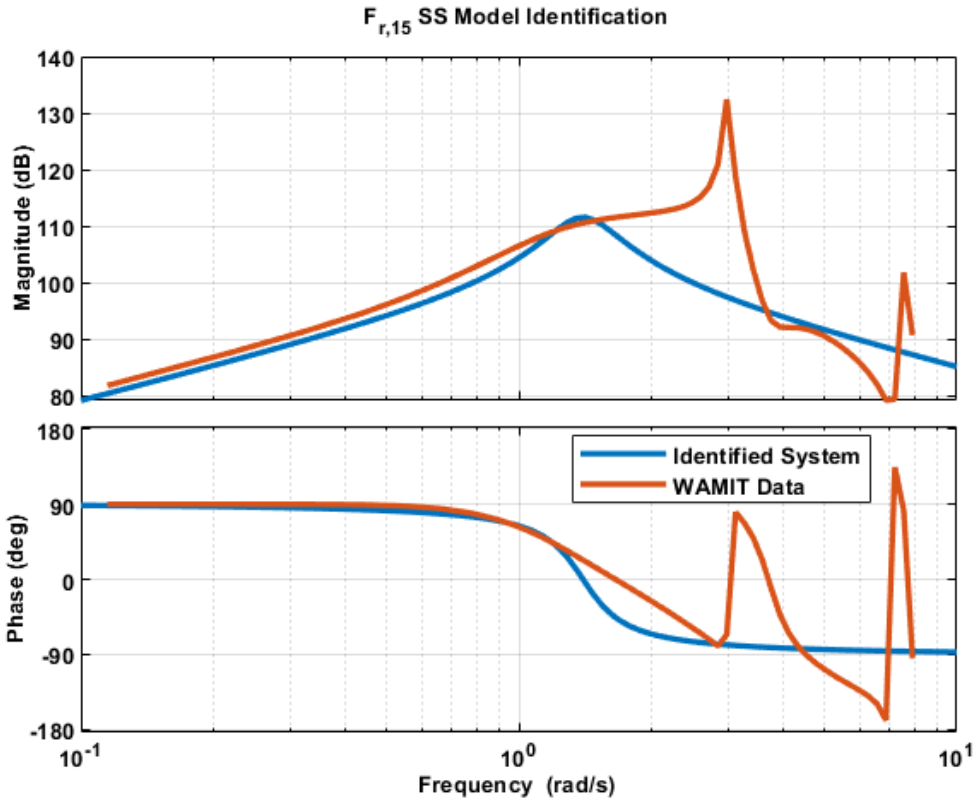

Figure 12. System Identification results, $F_{r,51}$(blue), frequency response data from BEMIO (brown).

```
Z51tf =

  From input "u1" to output:
       1.602e06 s
  ---------------------
  s^2 + 1.493 s + 5.347

Continuous-time transfer function.


Z51ss =

  A =
            x1       x2
   x1        0        1
   x2   -5.347   -1.493

  B =
              u1
   x1   1.282e+06
   x2  -1.913e+06

  C =
       x1  x2
   y1   1   0
```

Figure 13. Observer-canonical form of state-space description for $F_{r,51}$.

7.1.3.5. $F_{r,33}$ Radiation Force State-Space Model Identification

The system identification for the frequency response data object for $F_{r,33}$ constructed from BEMIO data is shown in Figure 14. The corresponding identified state-space model in the observer-canonical form is shown in Figure 15.

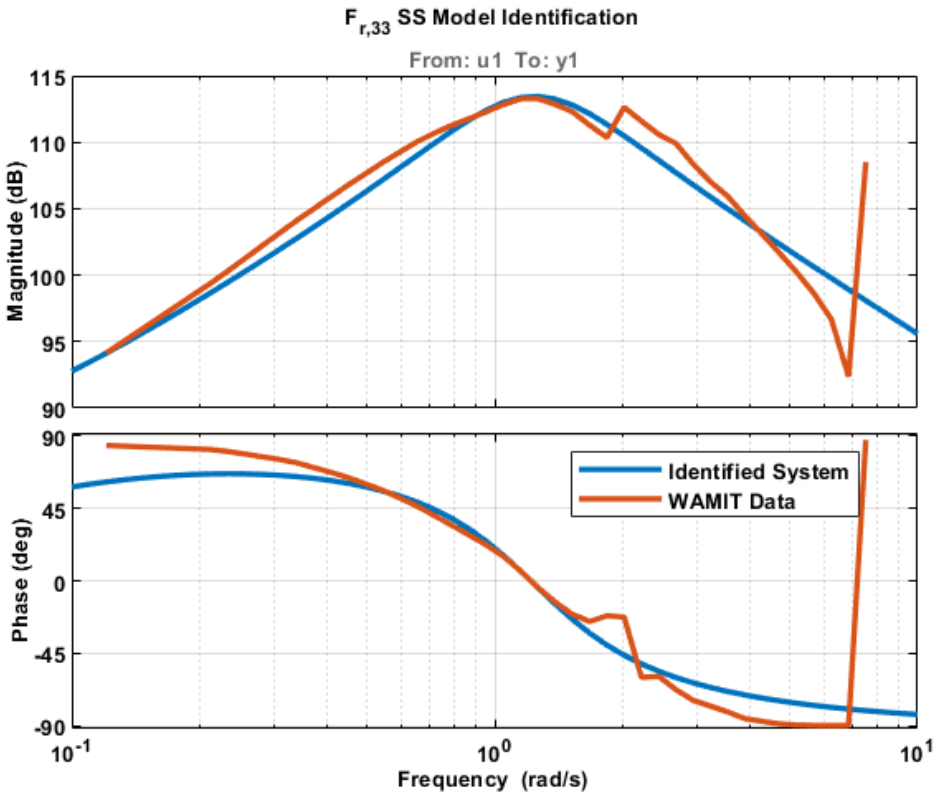

Figure 14. System Identification results, $F_{r,33}$(blue), frequency response data from BEMIO (brown).

```
z33ss =
  Continuous-time identified state-space model:
      dx/dt = A x(t) + B u(t) + K e(t)
       y(t) = C x(t) + D u(t) + e(t)

  A =
          x1      x2
   x1      0       1
   x2  -1.546   -1.27

  B =
              u1
   x1   5.976e+05
   x2  -7.287e+05

  C =
       x1  x2
   y1   1   0

  D =
       u1
   y1   0

  K =
       y1
   x1   0
   x2   0
```

Figure 15. Observer-canonical form of state-space description for $F_{r,33}$.

7.1.4. Nonquadratic WEC-PTO Model

The electrical power output from the PTO mechanism of the WEC is the difference between the mechanical power input from the waves and the losses in the PTO system. For a given PTO generator with a converter efficiency η_{Conv}, the copper loss constant K_{Cu}, and the winding resistance R_{Ω}, and i^{th} PTO current $I_{p,i}$, the electrical PTO power cost functional to be maximized, including the electrical losses, is given by,

$$\max_{F_{p,i}} P_{E,i} = \eta_{Conv}\left(F_{p,i}v_i - K_{Cu}I_{p,i}\left(F_{p,i}\right)^2 R_{\Omega}\right), \tag{23}$$

This case study scenario is taken from an example linear PTO generator [4] with the PTO force-current characteristics given by Figure 16(a). This relation is described by a third-order curve fit between the PTO current and the PTO force,

$$I_{p,i}\left(F_{p,i}\right) = a_{3,i}F_{p,i}^3 + a_{2,i}F_{p,i}^2 + a_{1,i}F_{p,i} + a_{0,i}, \tag{24}$$

Putting (24) in (23), we get,

$$P_{E,i} = c_{0,i}F_{p,i}v_i - (c_{1,i}F_{p,i}^6 + c_{2,i}F_{p,i}^5 + c_{3,i}F_{p,i}^4 + c_{4,i}F_{p,i}^3 + c_{5,i}F_{p,i}^2 + c_{6,i}F_{p,i} + c_{7,i}), \tag{25}$$

The surface plot of PTO cost functional in (25) is plotted in the PTO velocity-force plane, as shown in Figure 16(b).

7.1.5. NMPC Design for 2-DoF Heave-Pitch PTOs

A given NMPC problem optimizes a manipulated variable $\mathrm{u} \subseteq \mathrm{w}$ to maximize some cost functional P of a set of design variables w while respecting the given system constraints. A general class of NMPC problems has been formulated in [4], in which the cost functional takes on a nonlinear piecewise polynomial form. Considering the case of finite-horizon optimization, we can mathematically describe the NMPC problem of such a class as,

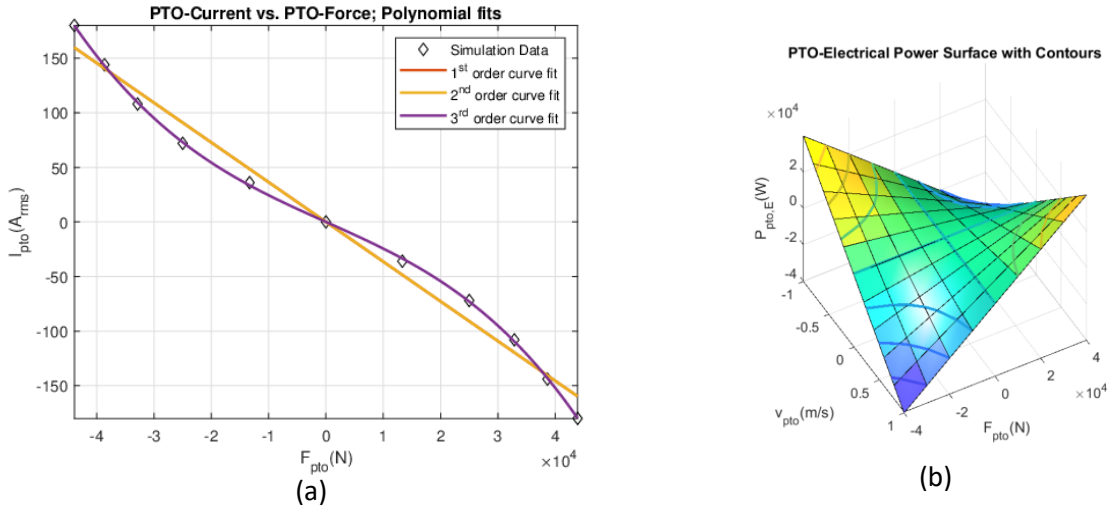

Figure 16. PTO current-force characteristics of PTO generator: (a) polynomial curve fitting for the experimental data; (b) electrical PTO power surface plot in PTO velocity-force plane.

$$\max_{\mathbf{u}} \mathbf{P}(\mathbf{w}) = \begin{cases} \mathbf{P_1}(\mathbf{w}) + \rho_{N,1}(\mathbf{w}), & w_k < R_1 \\ \mathbf{P_2}(\mathbf{w}) + \rho_{N,2}(\mathbf{w}), & R_1 \le w_k \le R_2 \\ \vdots & \vdots \\ \mathbf{P_j}(\mathbf{w}) + \rho_{N,j}(\mathbf{w}), & R_{j-1} \le w_k \le R_j \end{cases}, \tag{26}$$

subject to,

$$\text{Dynamic Constraints: } \dot{\mathbf{X}} = \mathbf{g}(\mathbf{w}), \tag{27a}$$

$$\text{Algebraic Constraints: } \mathbf{0} = \mathbf{p}(\mathbf{w}), \tag{27b}$$

$$\text{Equality Constraints: } \Upsilon_1 = \mathbf{B_{equal}}, \tag{27c}$$

$$\text{Inequality Constraints: } \mathbf{B_{lower}} \le \Upsilon_2 \le \mathbf{B_{upper}}. \tag{27d}$$

where, $w_k \in \mathbf{w}$ and Υ_i are algebraic expressions of the following forms,

$$\Upsilon_1 = \mathbf{\Psi_1 q}, \tag{28a}$$

$$\Upsilon_2 = \mathbf{\Psi_2 q}. \tag{28b}$$

For the 2-DoF (heave-pitch) WEC problem, the objective function to be maximized in (25) will be the sum of electrical PTO power output in the heave and pitch DoFs for each pod,

$$P_E = P_{E,3} + P_{E,5}, \tag{29}$$

Using the technique developed in [4], we can put (29) into Pseudo-Quadratic form by defining a suitable $\mathbf{h_i}$ vector for heave and pitch as,

$$\mathbf{h_i} = \begin{bmatrix} F_{p,i}^3 & F_{p,i}^2 & F_{p,i} & v_i & 1 \end{bmatrix}^T, \qquad i = 3,5 \tag{30}$$

with,

$$\mathbf{h} = \begin{bmatrix} \mathbf{h_3} \\ \mathbf{h_5} \end{bmatrix}, \tag{31}$$

we can reformulate (29) as,

$$P_E = \frac{1}{2}\mathbf{h}^{\mathbf{T}}\left(2\begin{bmatrix} \mathbf{W_3} & \mathbf{0} \\ \mathbf{0} & \mathbf{W_5} \end{bmatrix}\right)\mathbf{h} = \frac{1}{2}\mathbf{h}^{\mathbf{T}}(2\mathbf{W})\mathbf{h}, \tag{32}$$

By using (25) in (29), the weighting matrix $\mathbf{W}$ can be obtained by polynomial decomposition of (32) by the vector $\mathbf{h}$ in (31) as the basis vector,

$$\mathbf{W_i} = \frac{1}{2}\begin{bmatrix} -2c_{1,i} & -c_{2,i} & 0 & 0 & 0 \\ -c_{2,i} & -2c_{3,i} & -c_{4,i} & 0 & 0 \\ 0 & -c_{4,i} & -2c_{5,i} & c_{0,i} & -c_{6,i} \\ 0 & 0 & c_{0,i} & 0 & 0 \\ 0 & 0 & -c_{6,i} & 0 & -2c_{7,i} \end{bmatrix}, \quad i = 3,5 \tag{33}$$

7.1.6. Simulink Implementation of Pitch and Heave PTO NMPC

The Simulink model of 2-DoF NMPC for the pitch and heave is shown in Figure 18. The number of PTO units is increased in a step at 200 sec. The heave and pitch instantaneous PTO power and moving average power are shown in Figure 19 and 20, respectively. The heave and pitch PTO forces are shown in Figure 21 and Figure 22, respectively.

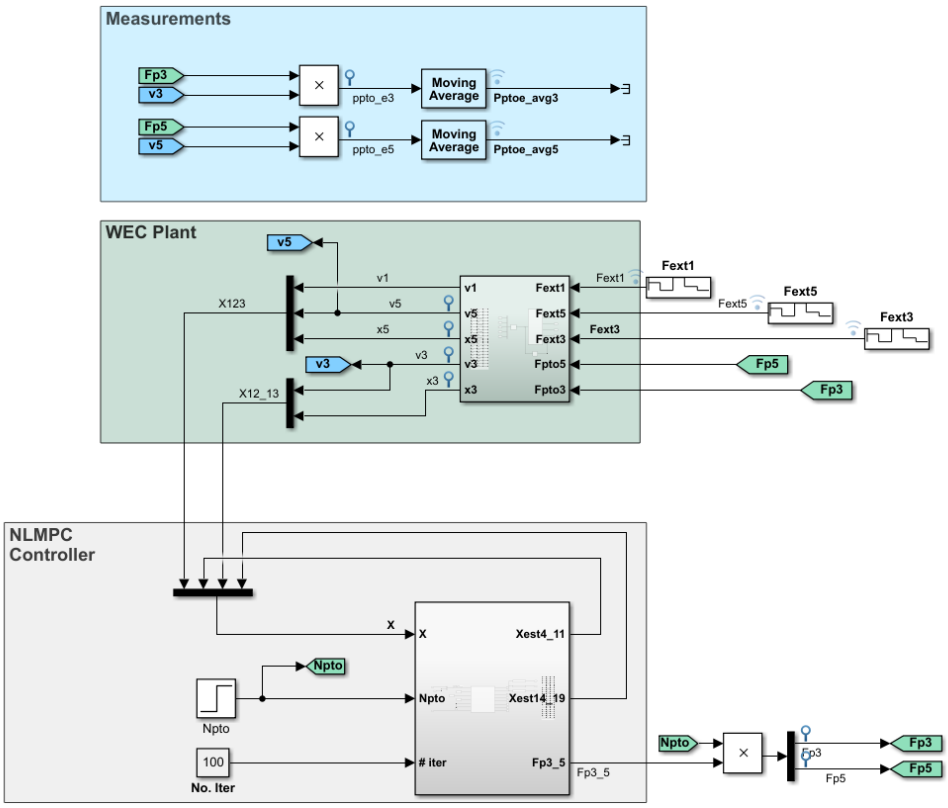

Figure 18. Simulink model of 2-DoF NMPC for a single pod.

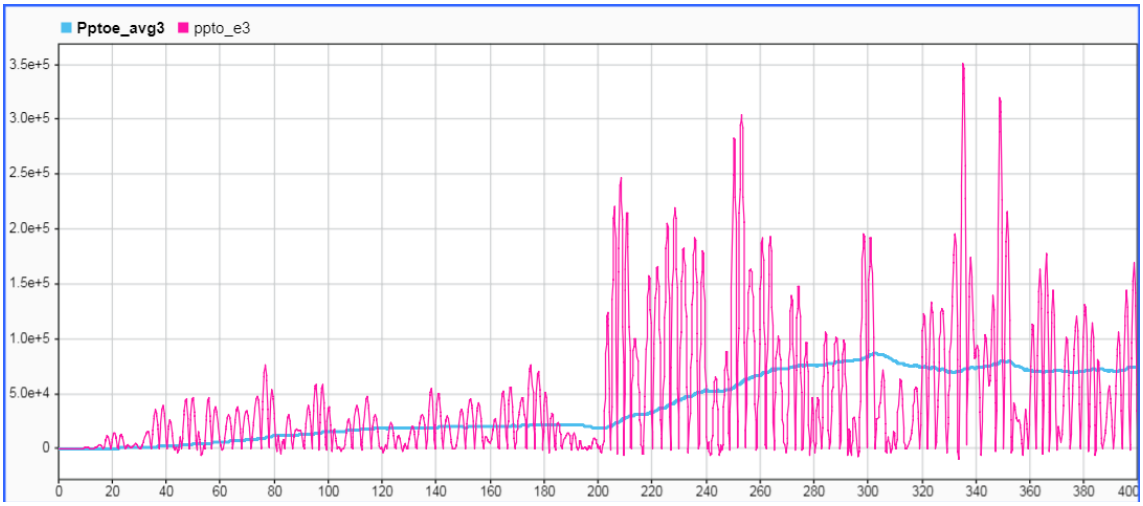

Figure 19. The heave PTO instantaneous power and moving average for a single pod.

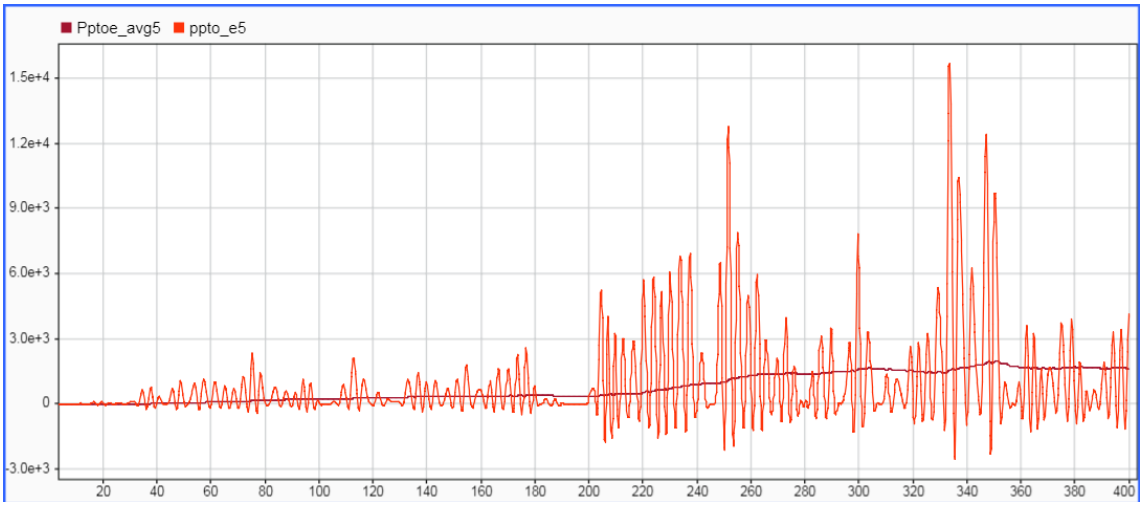

Figure 20. The pitch PTO instantaneous power and moving average for a single pod.

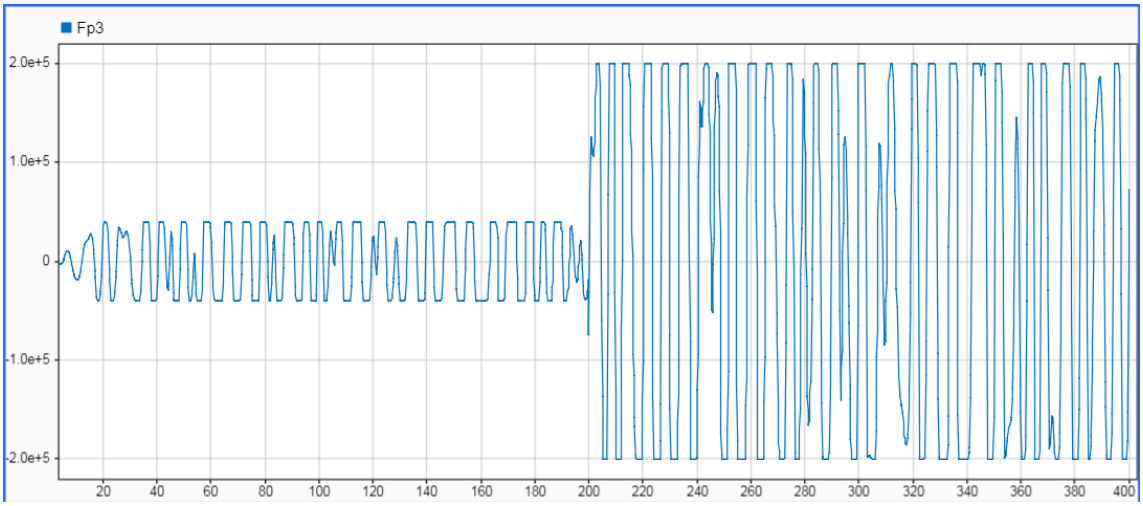

Figure 21. The heave PTO force for pod-1.

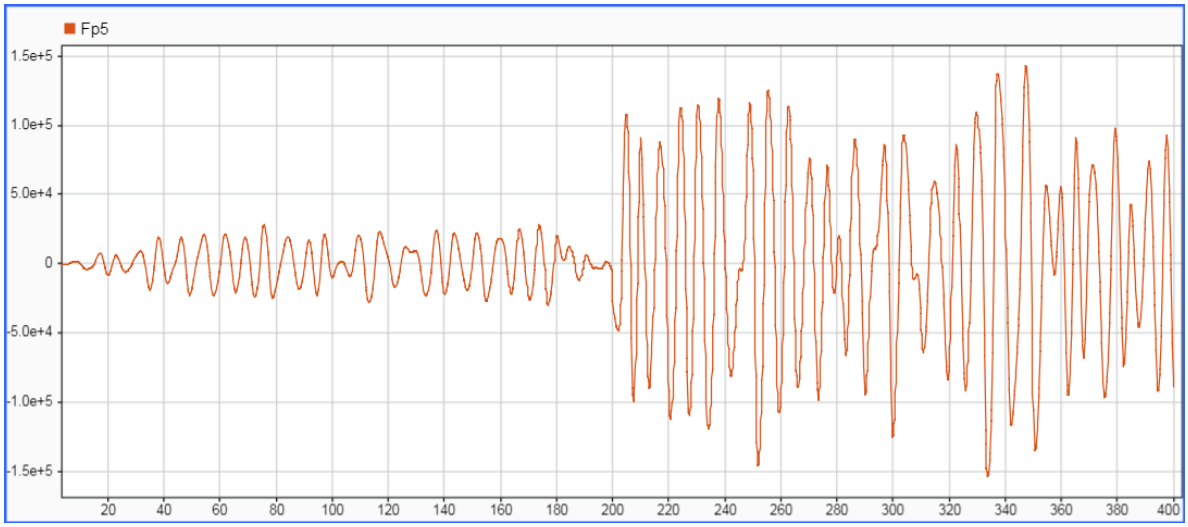

Figure 22. The pitch PTO moment for pod-1.

7.1.7. Interface of Pitch-Heave NMPC with a Single Pod in WEC-Sim Centipod Model

7.1.7.1 Heave-only-PTO WEC-Sim Model and Simulation with 2-DoF NMPC

The 2-DoF NMPC is interfaced with a single pod in the heave-only-PTO WEC-Sim model of Centipod shown in Figure 23.

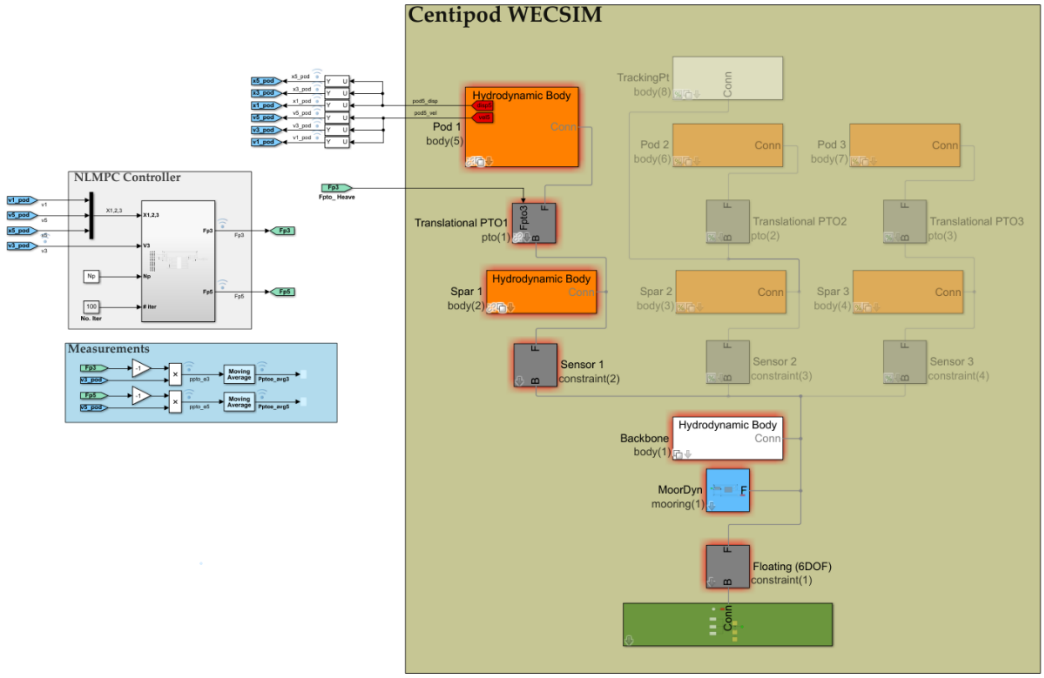

Figure 23. 2-DoF NMPC interface with WEC-Sim Single PTO model.

The simulation results for multiple PTO pickup coils are presented here. The instantaneous and moving average heave PTO power graphs are shown in Figure 24 under **Nonlinear** hydrodynamic conditions, the heave PTO force is shown in Figure 25, and the heave velocity and position for pod-1 are shown in Figure 26. The output power results under **Linear** hydrodynamic conditions are shown in Fig 27.

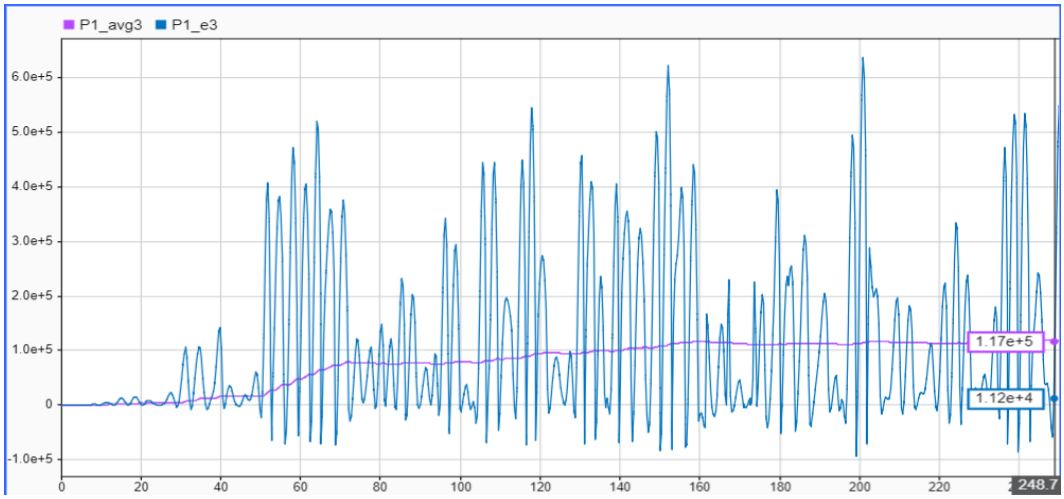

Figure 24. The heave PTO instantaneous power and moving average for a pod-1 in WEC-Sim under **Nonlinear** hydrodynamic conditions.

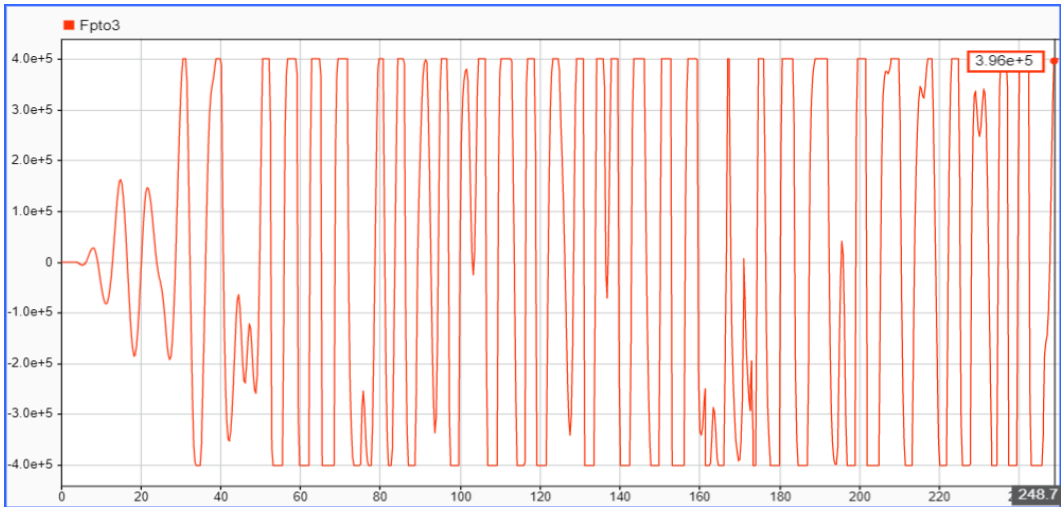

Figure 25. The heave PTO force for pod-1 under **Nonlinear** hydrodynamic conditions.

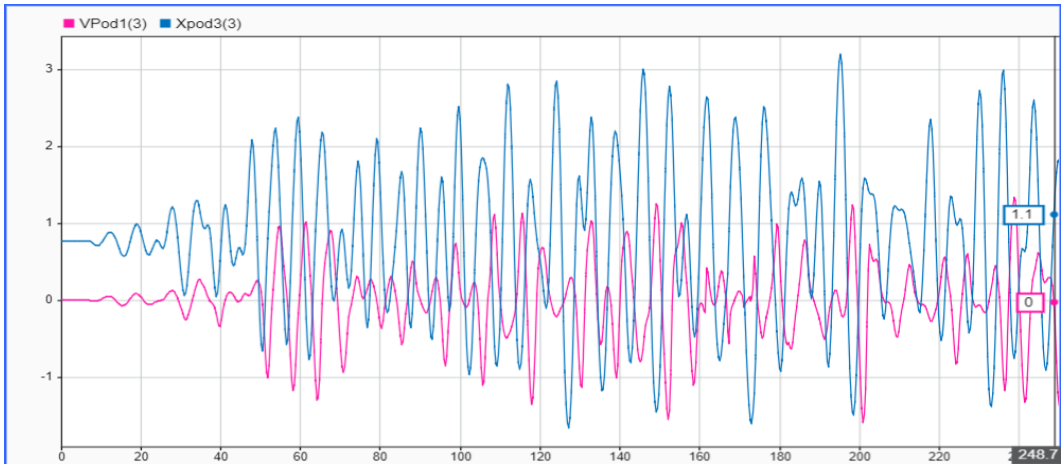

Figure 26. The heave velocity and position for pod-1 under **Nonlinear** hydrodynamic conditions.

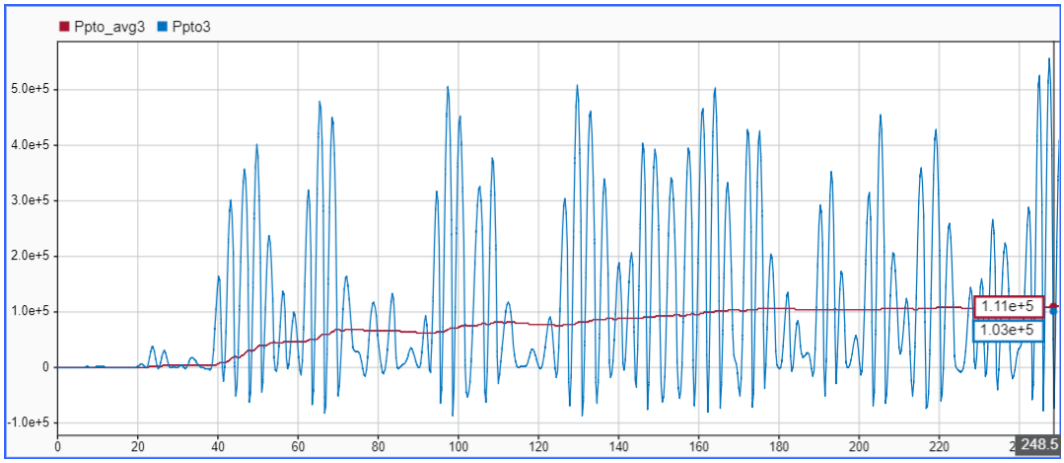

Figure 27. The heave PTO instantaneous power and moving average for a pod-1 in WEC-Sim under **Linear** hydrodynamic conditions.

7.1.7.2 Heave and Pitch-PTO WEC-Sim Model for Centipod and Simulation with 2-DoF NMPC

A pitch PTO is added in the WEC-Sim Centipod model along with the heave PTO mechanism, as shown in Figure 27.

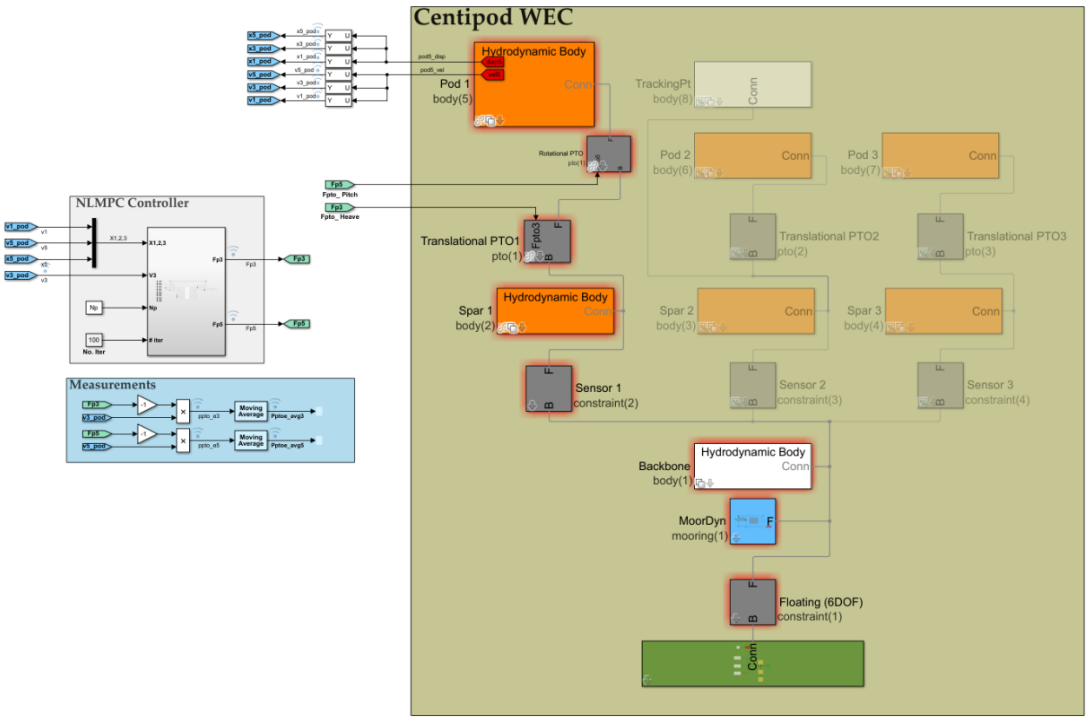

Figure 27. 2-DoF NMPC interface with WEC-Sim single PTO model with heave-pitch PTOs.

7.1.7.2.a Heave and Pitch Simultaneous Control

With the two degrees of freedom controller simultaneously in action for both degrees of freedom under **Nonlinear** hydrodynamic conditions, the instantaneous power and average power responses along with position and velocities are shown in Figure 29 through Figure 32 below. The output power results under **Linear** hydrodynamic conditions are shown in Figure 33 and Figure 34.

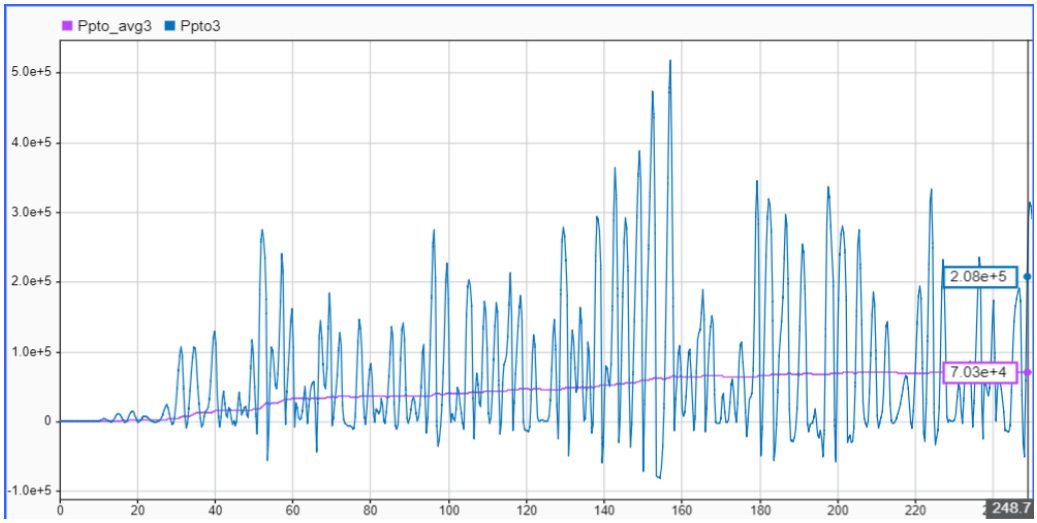

Figure 29. The heave PTO instantaneous power and moving average for WEC-Sim model for pod-1, under **Nonlinear** hydrodynamic conditions.

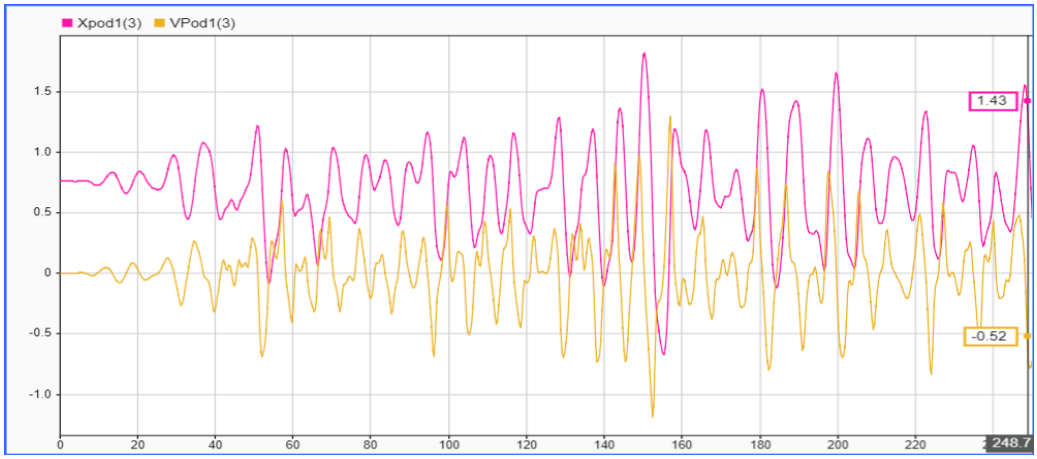

Figure 30. The heave velocity and position for pod-1.

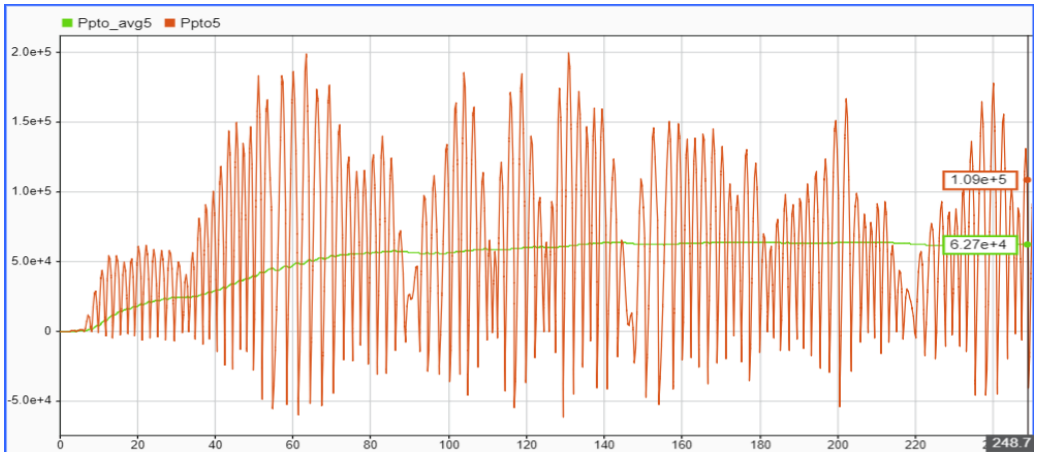

Figure 31. The pitch PTO instantaneous power and moving average for WEC-Sim model for pod-1, under **Nonlinear** hydrodynamic conditions.

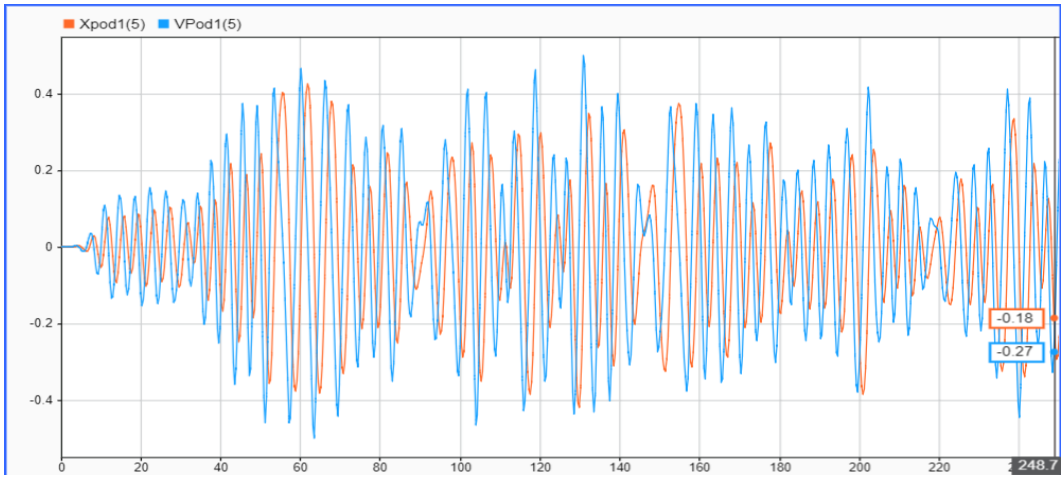

Figure 32. The pitch velocity and position for pod-1.

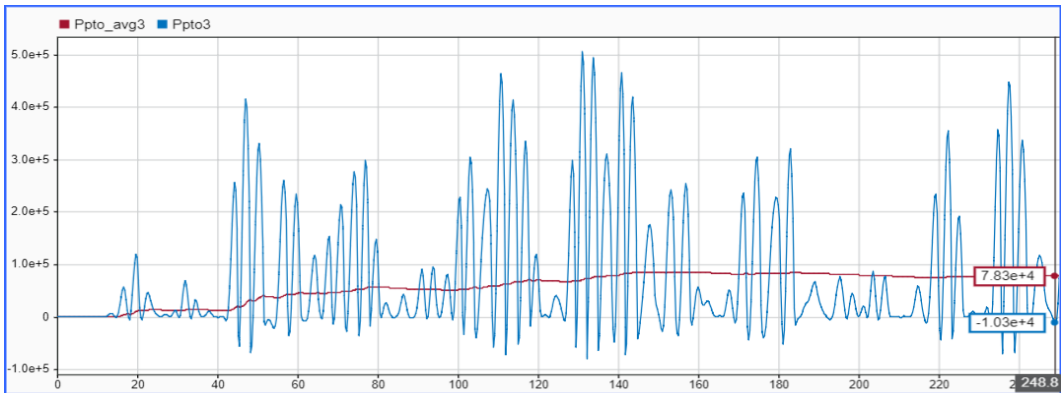

Figure 33. The heave PTO instantaneous power and moving average for WEC-Sim model for pod-1, under **Linear** hydrodynamic conditions.

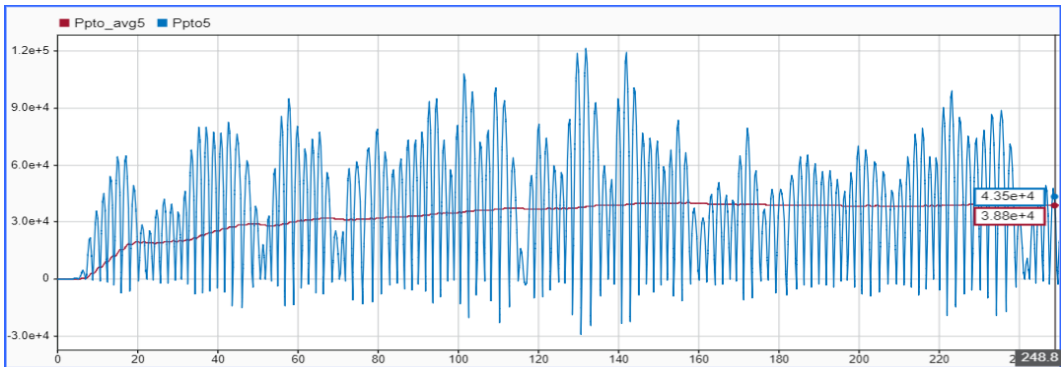

Figure 34. The pitch PTO instantaneous power and moving average for WEC-Sim model for pod-1, under **Linear** hydrodynamic conditions.

7.1.7.2.b Pitch Control Disabled, Heave Control Enabled System Responses

The heave output power responses under the scenario when the pitch control loop is open and the heave control loop is closed, are shown in Figure 35 and Figure 36 for nonlinear and linear hydrodynamics in WEC-Sim, respectively.

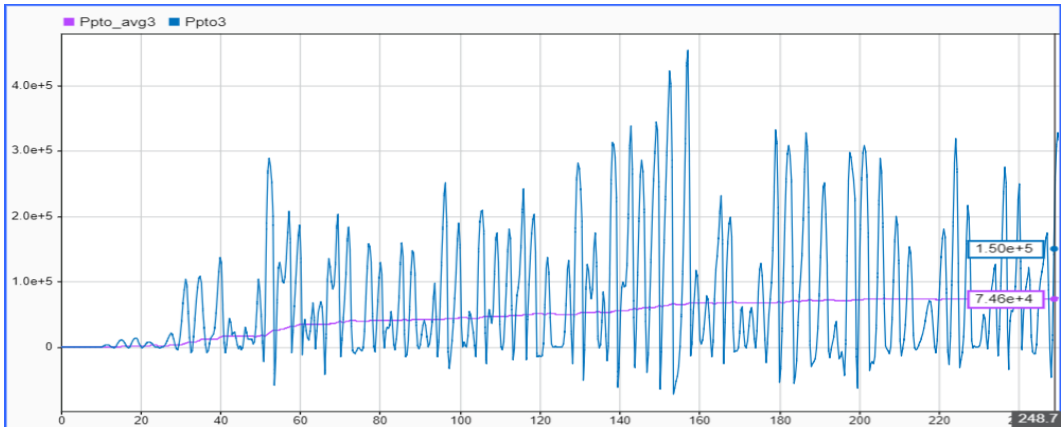

Figure 35. The heave PTO instantaneous power and moving average for WEC-Sim model for pod-1, under **Nonlinear** hydrodynamic conditions.

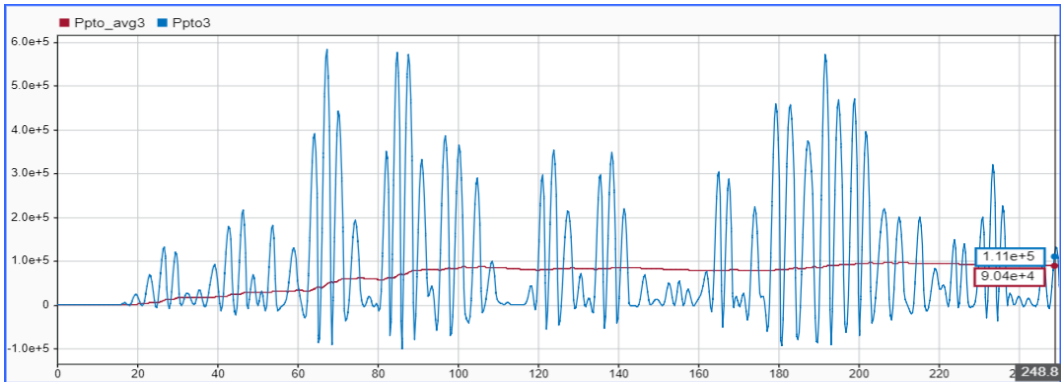

Figure 36. The heave PTO instantaneous power and moving average for WEC-Sim model for pod-1, under **Linear** hydrodynamic conditions.

7.1.7.2.c Pitch Control **Enabled**, Heave Control **Disabled** System Responses

The pitch output power responses under the scenario when the pitch control loop is closed and the heave control loop is open are shown in Figure 37 and Figure 38 for nonlinear and linear hydrodynamics in WEC-Sim, respectively.

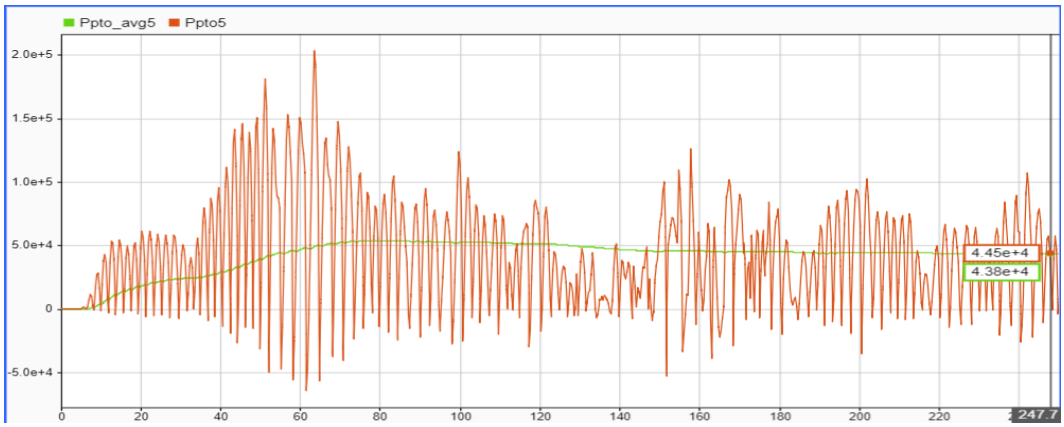

Figure 37. The pitch PTO instantaneous power and moving average for WEC-Sim model for pod-1, under **Nonlinear** hydrodynamic conditions.

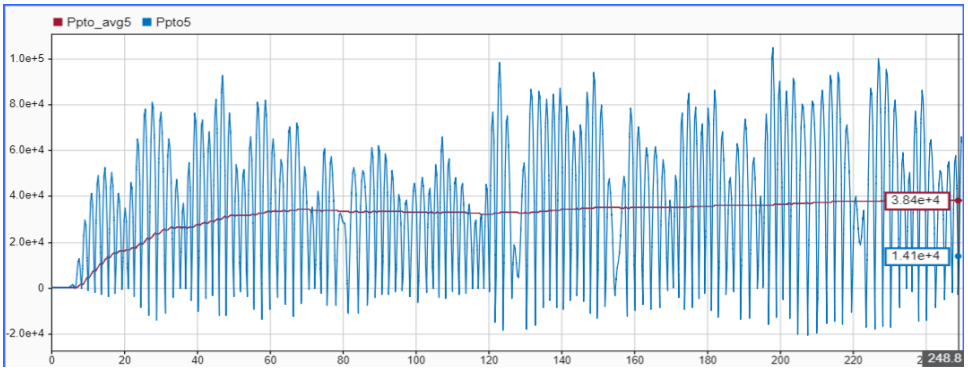

Figure 38. The pitch PTO instantaneous power and moving average for WEC-Sim model for pod-1, under **Linear** hydrodynamic conditions.

7.1.7.3 Pitch-only-PTO WEC-Sim Model and Simulation with 2-DoF NMPC

The 2-DoF NMPC is interfaced with a single pod in the pitch-only-PTO WEC-Sim. The pitch output power responses are shown in Figure 39 and Figure 40 for nonlinear and linear hydrodynamics in WEC-Sim, respectively.

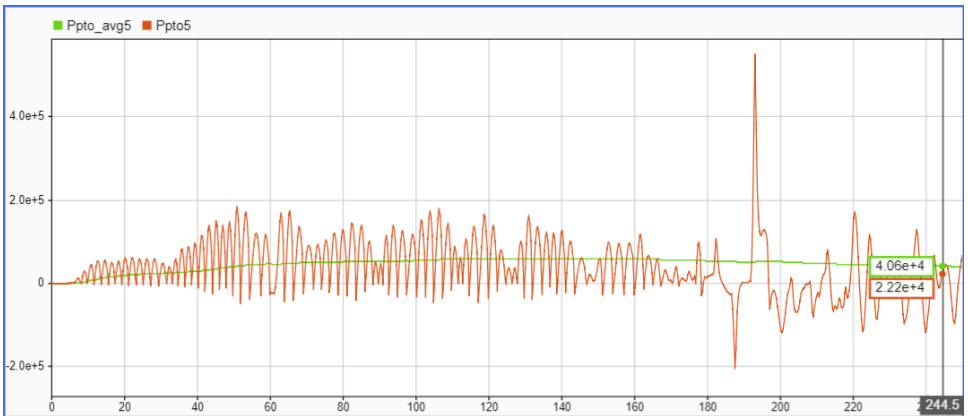

Figure 39. The pitch PTO instantaneous power and moving average for WEC-Sim model for pod-1, under **Nonlinear** hydrodynamic conditions; controller becomes unstable.

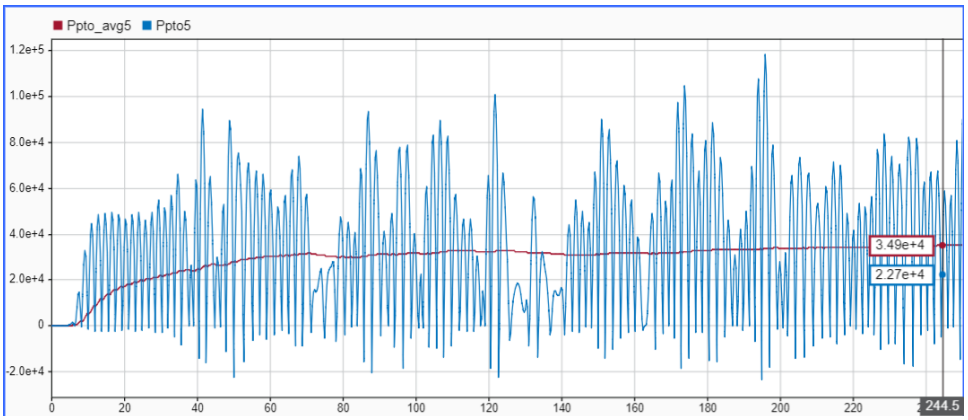

Figure 40. The pitch PTO instantaneous power and moving average for WEC-Sim model for pod-1, under **Linear** hydrodynamic conditions.

7.2 Lesson Learned and Test Plan Deviation

The summary of WEC-Sim simulation results for the full-scale version of Dehlsen's 3-pod device is given in Table 3 and Table 4 with the simulation conditions given in Table 1. For the average power results, the 'Exponential Weighting' option has been used to calculate the moving average of the instantaneous PTO power, with an exponential weight set to '1'; this selection gives equal weight to each data sample during averaging, and results get smooth with time, making them easy to be interpreted and compared. The data in Table. 2 corresponds to Linear hydrodynamic conditions in WEC-Sim while in Table. 3 corresponds to Nonlinear hydrodynamic conditions.

Table 1. Sea conditions for WEC-Sim simulation.

WEC-Sim Simulation Parameter	Value
Significant Wave Height [m]	2.5
Peak Period [s]	7.35
Wave Spectrum Type	Pierson Moskowitz (PM)
Wave Class	Irregular

Table 2. Average [1] output power results per Pod with *2-DoF NMPC* Controller, under *Linear* Hydrodynamic conditions in WEC-Sim

WEC DoFs	Controller Enabled	Reference Figures	Heave Power [kW]	Pitch Power [kW]	Net Power [kW]
One (Heave)	Heave	*27*	103.00	-	103.00
One (Pitch)	Pitch	*40*	-	34.90	34.90
Two (Heave and Pitch)	Heave	*36*	90.40	-	90.40
	Pitch	*38*	-	38.40	38.40
	Heave and Pitch	*33 and 34*	78.30	38.80	117.10

[1] Exponentially weighted moving average with exponential weight set to '1'.

Table 3. Average [2] output power results per Pod with *2-DoF NMPC* Controller, under *Nonlinear* Hydrodynamic conditions in WEC-Sim.

WEC DoFs	Controller Enabled	Reference Figures	Heave Power [kW]	Pitch Power [kW]	Net Power [kW]
One (Heave)	Heave	*24*	117.00	-	117.00
One (Pitch)	Pitch	*39*	-	Unstable	-
Two (Heave and Pitch)	Heave	*35*	74.60	-	74.60
	Pitch	*37*	-	43.80	43.80
	Heave and Pitch	*29 and 31*	70.30	62.70	133.00

[2] Exponentially weighted moving average with exponential weight set to '1'.

8 Conclusions and Recommendations

In moving from 1-DoF (heave) to 2-DoF (heave-pitch), the **power gain** for a single pod is **13.7%** for both, the linear and nonlinear hydro results in Table 2 and Table 2 respectively.The power gain per pod is calculated as follows,

$$\begin{aligned} \%\ \mathbf{Power\ Gain} &= \frac{(\mathbf{Net\ power\ with\ 2DoF}) - (\mathbf{net\ power\ with\ 1DoF\ Heave})}{\mathbf{net\ power\ with\ 1DoF\ Heave}} \times 100 \\ &= \frac{117.10 - 103.00}{103.00} \times 100 = 13.7\% \end{aligned} \tag{34}$$

The power gain result falls within the mean power improvement range anticipated for this project. While the result is reflective of only a single sea state, the improvement is likely to be reflected similarly in annual energy production (AEP), with an AEP uplift of over 10% expected. The AEP impact of this project will therefore have substantive impact on levelized cost of energy (LCOE), providing a justification for further pursuit of this line of research and continued work to integrate this DoF with the larger WEC design.

9 References

[1] "WEC-Sim (Wave Energy Converter SIMulator) — WEC-Sim documentation." https://wec-sim.github.io/WEC-Sim/ (accessed Mar. 27, 2021).

[2] J. van Rij, Y.-H. Yu, A. McCall, and R. G. Coe, "Extreme Load Computational Fluid Dynamics Analysis and Verification for a Multibody Wave Energy Converter," presented at the ASME 2019 38th International Conference on Ocean, Offshore and Arctic Engineering, Nov. 2019. doi: 10.1115/OMAE2019-96397.

[3] "Wamit, Inc. - The State of the Art in Wave Interaction Analysis." https://www.wamit.com/ (accessed Mar. 28, 2021).

[4] A. S. Haider, T. K. A. Brekken, and A. McCall, "A State-of-the-Art Strategy to Implement Nonlinear Model Predictive Controller with Non-Quadratic Piecewise Discontinuous Cost Index for Ocean Wave Energy Systems," in *2020 IEEE Energy Conversion Congress and Exposition (ECCE)*, Oct. 2020, pp. 1873–1878. doi: 10.1109/ECCE44975.2020.9235665.

10 Acknowledgements

Thank you to the TEAMER program and the U.S. Department of Energy Water Power Technologies Office (WPTO) for their support of this project.

11 Appendix

-